Ultracold Fermi-Fermi Mixtures of Lithium and Potassium

Dissertation

by

Frederik Matthias Spiegelhalder

submitted to the Faculty of Mathematics, Computer Science and Physics of the University of Innsbruck

in partial fulfillment of the requirements for the degree of doctor of science

advisor:
Univ. Prof. Dr. Rudolf Grimm,
Institut für Quantenoptik und Quanteninformation
Österreichische Akademie der Wissenschaften
Institut für Experimentalphysik
Universität Innsbruck

Innsbruck, February 2010

ABSTRACT

Ultracold atomic Fermi gases are a unique experimental tool for simulating and studying many-body systems. Since they are very well controllable and clean systems with tunable interactions, they can serve as quantum simulators for effects that occur in solid states and usually arise from the quantum nature of the Fermi gas of electrons. Different phenomena such as high-temperature superconductivity, Josephson junctions and ferromagnetism can be explored using degenerate Fermi gases. Even in the context of particle physics, Fermi gases can be used to simulate the behavior of quarks inside a nucleus.

In the past decade, experiments with a single fermionic (either ^{6}Li or ^{40}K) species have led to ground breaking results. In the past five years, several experiments have been set up that combine the two fermionic alkali species. Additionally to the capabilities offered by a single-species experiment (such as tuning of interaction strength, spin polarization, trap parameters), the two-species mixtures open up control of new parameters – the most obvious being the mass ratio. Due to the mass-imbalance, the Fermi-spheres would no longer overlap, and thus exotic quantum phases emerge. So far experimentally unobserved effects include superfluidity, phase separation, crystalline phases, exotic pairing mechanisms and long-lived trimers. More practically, a mixture would allow to species-selectively apply optical trapping potentials.

This thesis presents the experimental efforts from creating an ultracold Fermi-Fermi mixture of ^{6}Li and ^{40}K to the creation of heteronuclear molecules. Three published articles are contained in this thesis.

In the first article we report on the observation of Feshbach resonances in an ultracold mixture of two fermionic species, ^{6}Li and ^{40}K. The experimental data are interpreted using a simple asymptotic bound state model and full coupled channels calculations. This unambiguously assigns the observed resonances in terms of various *s*- and *p*-wave molecular states and fully characterizes the ground-state scattering properties in any combination of spin states.

In the second article we investigate the collisional stability of a sample of ^{40}K atoms immersed in a tunable spin mixture of ^{6}Li atoms. In this three-component Fermi-Fermi mixture, we find very low loss rates in a wide range of interactions as

long as molecule formation of ^{6}Li is avoided. The stable fermionic mixture with two resonantly interacting spin states of one species together with another species is a promising system for a broad variety of phenomena in few- and many-body quantum physics.

In the third article we present the essential experimental steps of our all-optical approach to prepare a double-degenerate Fermi-Fermi mixture of ^{6}Li and ^{40}K atoms, which then serves as a starting point for molecule formation. We first describe the optimized trap loading procedures, the internal-state preparation of the sample, and the combined evaporative and sympathetic cooling process. We then discuss the preparation of the sample near an interspecies Feshbach resonance, and we demonstrate the formation of heteronuclear molecules by a magnetic field ramp across the resonance.

CONTENTS

CHAPTER 1

INTRODUCTION

Almost all visible matter in the universe (in contrast to dark matter) is built up of up/down quarks, electrons and electron neutrinos. All of these elementary particles are fermions, i.e. they are particles with half-integer spin having anti-symmetric wave functions under exchange of identical particles. Combined, they form atoms which again can be fermions or composite bosons. Therefore, the physics of bosons can be regarded as a special case of fermion physics, where pairs are tightly bound and the fermionic character of the constituents is no longer relevant. This simple argument already shows that the physics of fermions is in general much richer than the physics of bosons.

In many areas of physics, interacting systems of fermions can be found, for example in condensed-matter physics (*e. g.* superconductors), in nulcear physics (protons and neutrons), in primordial matter (quark-gluon plasma), and even in astrophysics (white dwarfs and neutron stars). All these many-body systems are very challenging to describe theoretically. Therefore, ultracold Fermi gases with tunable interactions and controllable confinement are unique model systems for the experimental study of the rich physics of fermions.

Ultracold Fermi gases are very clean systems that can be controlled extremely well in the lab. Standard laser cooling and trapping techniques [Met99] are available for many years now and have become a tool for the exploration of a wide variety of physical phenomena. The ability to control the interaction of cold atoms by means of a magnetic Feshbach resonance have made it possible to access a regime called the *unitarity limit*: At resonance the scattering length diverges and the cross section reaches its maximum value $4\pi/k^2$, where k is the relative momentum of the scattering atoms. These properties are universal because they are independent of any feature of atomic potentials [Ho04]. Therefore ultracold atoms very close to a Feshbach resonance share the same universal properties as other quantum many-body systems such as a neutron star or an electron gas in condensed matter. For reviews about Feshbach resonances see for example [Chi10, Köh06, Tim99]. For a review about ultracold Fermi gases see [Ing08, Gio08] and references therein.

This Chapter gives a brief introduction into the field of ultracold Fermi gases. In

Section 1.1 the development of single-species experiments is shortly reviewed. In Section 1.2 an overview is given of the recent development of experiments with mixtures of two fermionic species and some theoretical proposals, promising rich and new physics, are presented. Section 1.3 gives an overview of the content of this thesis. Finally, Section 1.4 gives an outlook over the currently ongoing measurements in the Innsbruck FeLiKx (Fermionic Li-K experiment) experiment. In Appendix A schematic drawings of the cooling and imaging frequencies used in the experiment are documented.

1.1. Single Species

The field of ultracold Fermi gases is rapidly expanding. Worldwide more than 13 groups have reported creation of degenerate Fermi gases with the most common species being the two naturally abundant alkali metal fermionic isotopes ^{6}Li and ^{40}K. Apart from those two elements, degenerate Fermi gases have been created from ^{3}He* [McN06] and ^{173}Yb [Fuk07]. After the creation of a Bose-Einstein codensate (BEC) of ^{84}Sr [Ste09, Esc09], creation of the first quantum degenerate Fermi gas of an earth alkaline metal (^{87}Sr) is at reach.

The scattering of atoms is described by the scattering phase and the angular momentum quantum number l. For a derivation of basic scattering theory see a textbook or review [CT77, Ing99]. At very low energies, collisions can occur only with the lowest $l = 0, 1, 2, ...$ called s, p, d-wave scattering. In a gas of identical fermions, due to the anti-symmetric wave function, only odd partial waves (odd l) contribute to the scattering process. However, in an ultracold gas, the contribution of higher partial waves is frozen out and thus the dominant scattering process is s-wave scattering. In a system of identical fermions, s-wave scattering is prohibited. Therefore the behavior of such a gas is collisionless, which means that the atoms freely move in the trap without scattering. Bosonic atoms exhibit a different dynamic behavior since s-wave scattering is allowed. Depending on the scattering rate of the atoms, a Bose gas shows either collisionless or hydrodynamic behavior. Hydrodynamic behavior means that the gas behaves like a fluid under free expansion. This happens either when the scattering rate is very high or when the gas becomes superfluid. A BEC shows superfluid hydrodynamic behavior.

Since identical fermions cannot undergo s-wave collisions, ultracold Fermi gases of a single species are usually prepared as a mixture of two internal spin states. This leads to a rich dynamic behavior of the gas. It allows for s-wave scattering between different spin states and continuous tuning of the scattering length by means of a Feshbach resonance. Also in a mixture of two spin states the Pauli exclusion principal plays an important role. Although s-wave collisions are allowed between different atomic states, the available phase space for scattering is reduced if the Fermi gas is degenerate. This reduces the scattering rate and eventually leads again to collisionless behavior of the gas.

Formation of pairs can dramatically change the dynamic behavior of the gas. One pairing mechanism is the formation of molecules. Here we consider a very weakly bound molecular state where the binding energy can be tuned using an external

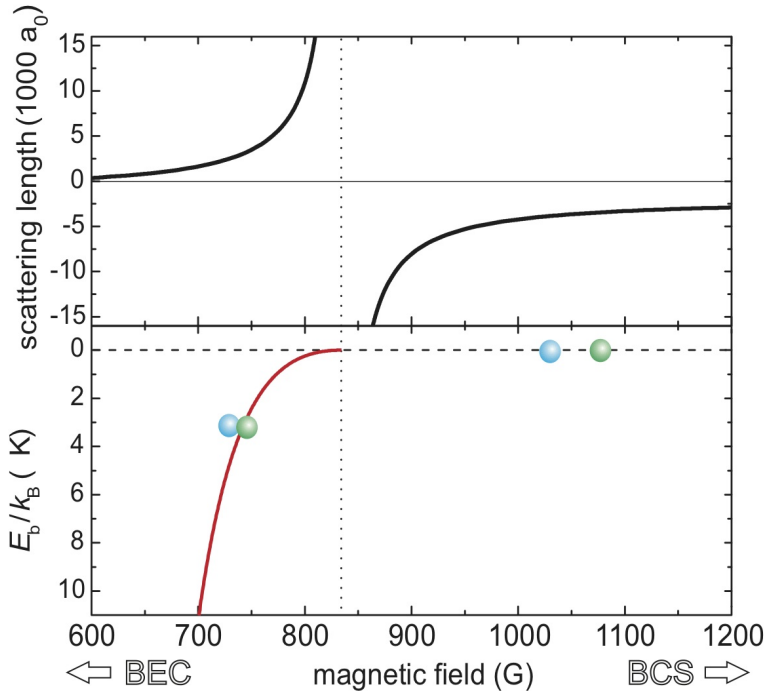

Figure 1.1. The upper panel shows the s-wave scattering length between ^{6}Li atoms in the lowest two energy states for magnetic fields close to the 834 G-Feshbach resonance [Bar05]. The resonant behavior of the scattering length comes along with a weakly bound molecular state which connects to the free atom continuum at the position of the Feshbach resonance. The lower panel shows the binding energy divided by the Boltzmann constant E_b/k_B of this molecular state. The fact that the molecular state is connected to the free atom continuum allows to adiabatically convert the fermionic atoms into bosonic molecules. Furthermore the Feshbach resonance smoothly connects the molecular BEC regime with the BCS regime.

magnetic field; see Fig. 1.1. Close to a Feshbach resonance, the scattering length directly depends on the binding energy of the molecular state [Chi10]. The center of the Feshbach resonance is located at the magnetic field where the molecular state reaches the energy continuum of free atoms. Beyond the point where the molecular state reaches the atom continuum, pairing is still possible by a many-body mechanism described by Cooper [Coo56]; these pairs are therefore called Cooper pairs. Due to the Cooper pairs, the gas becomes superfluid at low temperature when a Bardeen-Cooper-Schrieffer (BCS) superfluid forms [Bar57b, Bar57a]. Close to the Feshbach resonance, where the gas cannot be considered as dilute, the nature of the strongly interacting pairs is more complex than simple molecules or Cooper pairs. The pairing mechanisms are illustrated schematically in Fig. 1.2.

With decreasing temperature, superfluid behavior of the system emerges. On the BEC-side of a Feshbach resonance, two fermions form a composite boson and a molecular BEC forms [Joc03, Gre03, Reg03a, Zwi03]. On the BCS-side of the resonance, many-body pairing makes the gas become superfluid at low temperature when a Bardeen-Cooper-Schrieffer (BCS) superfluid forms [Bar57b, Bar57a]. These two regimes are smoothly connected via the Feshbach resonance by changing the

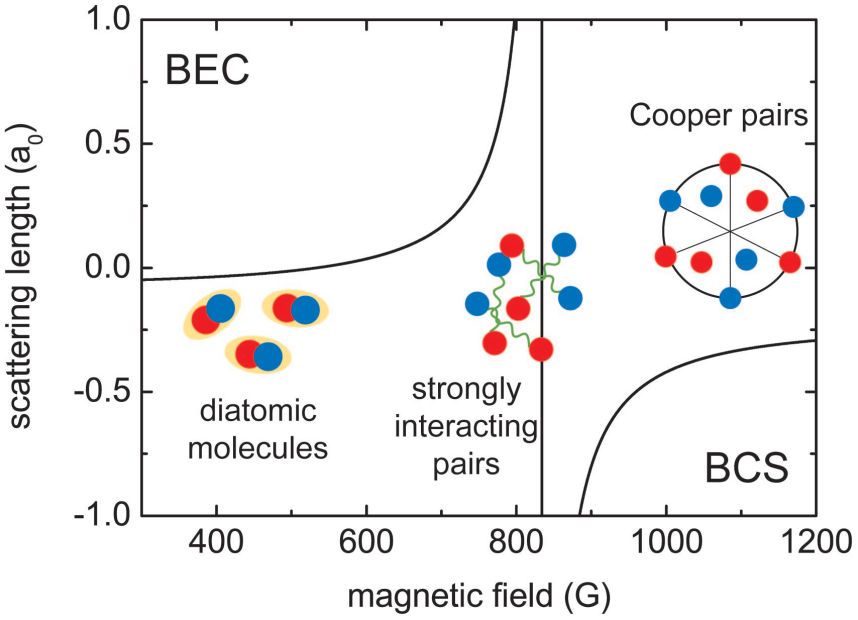

Figure 1.2. Illustration of the BEC-BCS crossover. Shown is the Li 834-G Feshbach resonance and schematic images of the pairing mechanisms on the BEC-side of the resonance, in the unitarity regime and on the BCS-side of the resonance. On the BEC side of the resonance, diatomic molecules form, while on the BCS side, pairing occurs in momentum space and is a many-body effect. In the unitarity regime right on resonance, the pair size is comparable to the interatomic distance.

magnetic field. The intermediate region between the BEC and the BCS regime is called the BEC-BCS crossover region [Eag69, Leg80, Noz85, Eng97]. In this region the scattering length exceeds the interparticle spacing and therefore the gas cannot be considered as dilute anymore. In this region we can observe a strongly interacting Fermi gas.

Since the first experiments reporting on quantum degenerate Fermi gases in 2001 [Sch01] and 2002 [O'H02], there has been tremendous progress in experiments investigating strongly interacting Fermi gases. The first experiments focused on the realization of pair condensates both in the molecular regime [Joc03, Gre03, Reg03a, Str03, Zwi03] and on the BCS side of the Feshbach resonance [Reg04, Zwi04, Zwi05b]. Measurements of the cloud size [Bar04] and the expansion of the cloud [Bou04] showed that there is a smooth crossover from the BEC to the BCS regime. Using radio frequency (rf) spectroscopy, several experiments were performed to study the pairing gap [Chi04, Shi07, Sch08a], the size of the pairs [Sch08b], and single-particle excitations [Ste08]. Pairing throughout the crossover was further studied using optical molecular spectroscopy [Par05]. The excitation spectrum was investigated using a magnetic field modulation technique [Gre05]. Thermodynamic properties like the heat capacity [Kin05] and the entropy [Luo07] were measured. The momentum distribution of the gas in the crossover regime was studied using expansion measurements both in the low temperature limit [Reg05b] and as a func-

tion of the temperature [Che06a]. The potential energy of the gas was determined by measuring its expansion [Ste06]. The first experimental measurements of the equation of state of a uniform gas have been reported by [Nas09] together with a detailed comparison with existing theories. Recent experiments applied Bragg spectroscopy to probe the dynamic and static structure factor [Vee08] and thus are able to determine the critical temperature using fast magnetic field ramps [Ina08].

The entropy of a trapped Fermi gas with resonant interactions was calculated by [Che05a]. Experimentally it is very difficult to measure such quantities of a strongly interacting gas. Usually, a way to determine the temperature of an ultracold gas would be fitting a Thomas-Fermi profile to the density distribution measured after free expansion. In practice this can be very complicated since most of the information about the temperature is hidden in the wings of the density distribution, right where absorption images can be very noisy. Therefore it would be very useful to have a weakly interacting probe, that can be treated as a classical gas which is in thermal contact with the strongly interacting gas. In Chapter 3 we present such a method, which also inspired the group from Paris to use ^{7}Li as a temperature probe for ^{6}Li [Nas09].

A very powerful tool for measuring the dynamic behavior of strongly interacting Fermi gases is the observation of collective oscillations. The frequency and damping of different oscillatory modes can give insight in the pairing mechanism at different interaction strength across the BEC-BCS crossover. This way it was possible to perform high-precision measurements and observe the transition from hydrodynamic behavior at low temperature to collisionless behavior at higher temperature and compare the result to theoretical model calculations. Different collective modes such as sloshing modes, compression modes, quadrupole modes and the scissors mode have been used (see [Rie08] and references therein).

The dynamic behavior of the strongly interacting gas was also studied by measuring the sound velocity [Jos07] and investigating irrotational flow during expansion [Cla07]. A direct proof of superfluidity of the crossover gas was gained by the formation and observation of a vortex lattice [Zwi05a]. In subsequent experiments the behavior of the superfluid gas under expansion [Sch07] and the critical velocity for superfluid flow was explored [Mil07].

One of the current hot topics in single species experiments is the behavior of imbalanced Fermi gases. When the two populations of fermions are unequal, not every particle can find a partner, raising the question of whether superfluidity can persist in response to such a population imbalance. Already in 1962, Chandrasekhar and Clogston predicted an upper limit for the magnetic field, beyond which superconductivity with equal spin densities will break down [Clo62, Cha62]. Fulde and Ferrell [Ful64], and independently Larkin and Ovchinnikov [Lar65], proposed a more stable configuration of the superconductor that allows for unequal densities, the FFLO or LOFF state containing nonzero-momentum Cooper pairs. First experimental observation of phase separation between a superfluid paired core and a polarized shell in an imbalanced Fermi gas was reported in 2006 [Par06, Shi06]. Of particular interest is the phase transition between the superfluid and the normal phase and whether it is of first or second order [Sar63]. The superfluid regime of

the imbalanced gas has been mapped out for a broad range of spin imbalance and interaction strength [Zwi06]. In particular, the intermediate phase in the transition between the paired core and polarized shell yields interesting effects like the formation of fermionic quasiparticles known as polarons [Sch09, Nas09] that have also been described theoretically [Lob06, Che06b, Com08, Pro08]. The Fermi polaron consists of an impurity immersed in a noninteracting Fermi sea analogous to the condensed matter case of an electron immersed in a bath of noninteracting (bosonic) phonons. Another famous example of an impurity problem is the Kondo effect [Kon64], where an enhanced resistance in metals is caused by immobile spin impurities.

Recently, experiments on three-state Fermi gases investigated the collisional stability in the strongly interacting regime [Ott08, Huc09].

1.2. Heteronuclear Mixtures

In recent years several groups around the world (Amsterdam, Innsbruck, MIT, Munich and Paris in alphabetical order) have started to set up experiments on mixtures of two different fermionic species. These heteronuclear mixtures have gained a lot of interest due to additional parameters inaccessible in single-species experiments. Combining two different elements leads to a mass-imbalanced system. Furthermore, a heteronuclear mixture allows to apply species-selective trapping potentials [LeB07]. By confining one species in one or two dimensions using an optical lattice that does not interact with the three-dimensional background Fermi-sea of the other species it is possible to introduce a so-called mixed dimensionality, leading to very rich physics as will be described in more detail in Section 1.2.2.

In the following two Sections, the current experimental situation will be presented and an overview of theoretical proposals that are relevant for future experiments will be given.

1.2.1. Experiments

Figure 1.3 shows the atomic ground-state energy structure of ^{6}Li and ^{40}K. For simplicity we label the energy levels Li$|i\rangle$ and K$|j\rangle$, counting the states with rising energy. This notation is used throughout this thesis.

The first experimental team that was able to cool down a Fermi-Fermi mixture to quantum degeneracy, was the Munich group [Tag08]. Bosonic ^{87}Rb was used as a coolant, allowing them to obtain 1.8×10^5 atoms of each species at degeneracies of $T/T_F \leq 0.4$. This degenerate and balanced mixture also served as the starting point for the first observation of heteronuclear molecules made from fermionic ^{6}Li and ^{40}K [Voi09].

Shortly after the Munich group had achieved quantum degeneracy of the ^{6}Li-^{40}K mixture, we presented our first results on the interspecies Feshbach resonances [Wil08]. A total of 13 s- and p-wave resonances in different spin channels was observed at magnetic fields up to 1000 G and assigned with the help of our collaborators (Tobias Tiecke and Jook Walraven from the University of Amsterdam, Servaas

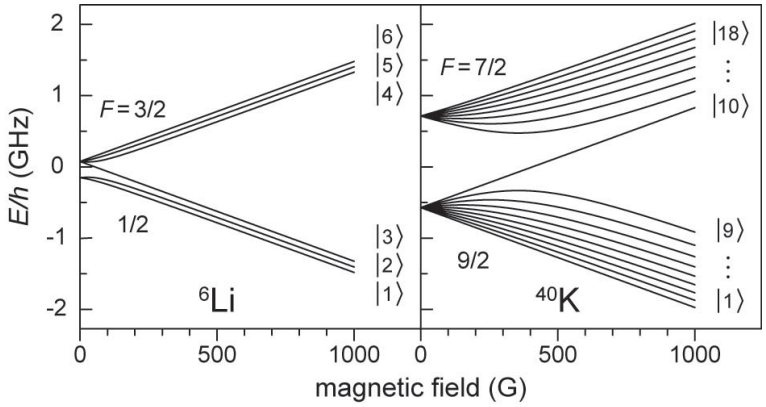

Figure 1.3. Electronic ground state energies of ^{6}Li and ^{40}K versus magnetic field.

Kokkelmans from TU Eindhoven and Eite Tiesinga and Paul Julienne from NIST). We characterized the interaction properties of the mixture by means of Feshbach spectroscopy and two theoretical models. All *s*-wave resonances observed are rather narrow and thus closed-channel dominated.

In Amsterdam another experimental team is working with an ultracold mixture of ^{6}Li and ^{40}K. They evaporate their mixture in an optically plugged magnetic trap. A mixture of Li in the fully stretched state $|6\rangle$ is combined with a three state mixture of K in the states $|8\rangle$, $|9\rangle$ and $|10\rangle$. Since K is the element which is evaporated, the three state mixture assures effective thermalization. Li is sympathetically cooled by K. After forced evaporation in the magnetic trap they load their sample into an optical trap and transfer all atoms into the lower hyperfine state.

Together with their collaborators from Eindhoven, the Amsterdam group developed a computationally light model for assigning Feshbach resonances. This so-called Asymptotic Bound-State model (ABM), was used in Ref. [Wil08] to identify the13 observed interspecies Feshbach resonances. With the ABM it is also possible to calculate the widths of Feshbach resonances and the Amsterdam group was able to identify the broadest resonances in the mixture of Li in the absolute ground state with K in higher spin states [Tie10]. In the Li$|1\rangle$K$|10\rangle$ channel they could also experimentally determine the widths of the Feshbach resonance by finding the zero crossing of the *s*-wave scattering length. The measured width of 1.5 G is comparable with the calculated with of 0.9 G. The theoretical value is known to slightly underestimate the actual width [Tie09]. It is of great importance to find out which spin channel yields a strong Feshbach resonance with a width that makes it experimentally feasible to access the strongly-interacting regime.

In comparison, all three experiments on heteronuclear Fermi-Fermi mixtures, follow slightly different approaches in order to reach ultracold mixtures. The Munich group can achieve much higher atom numbers than the Innsbruck experiment, with equal amounts of about 1.8×10^5 in each species at quantum degeneracy. Both, the Amsterdam and the Innsbruck experiments, use one of the fermionic species for sympathetic cooling of the other species. In Amsterdam the coolant is K, while in Innsbruck the coolant is Li. This way, both experiments end up with a ratio of

about 10:1 in atom number of the coolant species to the sympathetically cooled species. Thus, in Innsbruck we have a minority component of K immersed in a much larger sample of Li atoms. In Amsterdam a minority of Li atoms is immersed in a large sample of K.

The further steps in the field of heteronuclear Fermi-Fermi mixtures will include the probing of the strongly interacting regime at an interspecies Feshbach resonance. The 155-G Feshbach resonance in the Li$|1\rangle$K$|3\rangle$ channel, which has a width of about 0.8 G, is a promising candidate for achieving high enough scattering lengths in order to enter the strongly interacting regime. First measurements on collective oscillations close to the resonance have been performed in Innsbruck and have proven to be a powerful tool for localizing the zero crossing of the scattering length [Nai10].

A very promising route for exploring new and interesting many-body effects is the implementation of mixed-dimensionality into the ^{6}Li-^{40}K system. For example. the minority component of the mixture, in our case K, could be confined in a lower-dimensional trap while immersed inside a background Fermi sea of Li in a shallow trap. In the next Section several theoretical proposals are presented that promise rich physics arising from such mixed-dimensional systems.

Additionally to the Fermi-Fermi mixtures, it is also possible and very interesting to study Bose-Fermi mixtures. Both Li and K have bosonic isotopes, namely ^{7}Li and ^{39}K, which have high natural abundances and are technically easy to implement by simply changing the laser detuning.

1.2.2. Theoretical Proposals

Especially in the field of condensed matter physics, Fermi gases may prove to be unique tools to study many-body effects that are unaccessible otherwise. The ability to tune the interactions and prepare well-controllable and clean systems makes exotic phases observable, some of which have been theoretically suggested decades ago. Perhaps one of the most interesting of a number of exotic polarized superconducting phases is that proposed over 40 years ago and is now known as the FFLO phase. Tho original concept by Fulde and Farrell is based on the formation of cooper pairs with nonzero centre of mass momentum [Ful64]. In a related model, Larkin and Ovchinnikov describe an oscillating superconducting oder parameter [Lar65]. Since then, the theoretical models have been under a lot of development [Cas04]. More recently, theorists consider ultracold trapped Fermi gases and describe how the FFLO phase could be observed in such systems [Edg09]. An experimental group at Rice University has reported first possible experimental observation [Lia09].

In the following an overview of theoretical proposals relevant for the field of heteronuclear Fermi-Fermi mixtures is given.

In the heteronuclear mixtures, exotic pairing mechanisms such as breached-pair superfluidity are expected [For05]. Furthermore, in systems of large mass-imbalance, crystalline phases could be observed [Pet07]. Quantitative predictions for phase separation between a normal and a superfluid phase for a unitary Fermi

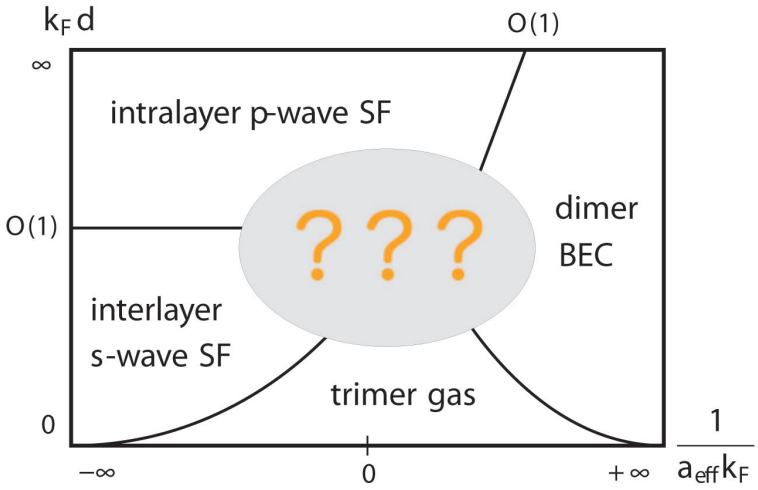

Figure 1.4. Phase diagram mixed dimensions. The four indicated phases are illustrated schematically in Fig. 1.5. What happens at the center of the phase diagram is unknown.

gas with population imbalance and unequal masses are given in Ref. [Bau09]. Superfluid paring between fermions of unequal masses is the topic of another theory paper [Bar08]. Restricting the mixture to a quasi-two-dimensional geometry would allow for stable weakly bound trimers with unit angular momentum [Lev09]. A peculiar atom-dimer p-wave resonance occurs, whose interaction can be tuned from attractive to repulsive by changing the frequency of the confinement.

Since the mixture of two species allows to create trapping potentials which are species-selective [LeB07], it is possible to combine confinement in different dimensions. For example, one species could be confined in a two-dimensional plane or one-dimensional line, while the other species is free in the three-dimensional space. Several theoretical articles have presented these mixed-dimensional systems also for the case of ^{6}Li-^{40}K [Nis09a, Nis09b, Nis08]. By confining the heavier K in two dimensions while Li is free in three dimensions, very rich physics can arise. In the case of a two-layer combination, formed by a one-dimensional optical lattice for the K atoms, together with the free background Fermi sea, four interesting regions arise in the phase diagram depicted in Fig. 1.4. Depending on the interlayer separation d, the effective scattering length a_{eff} and the interparticle distance characterized by k_F, different many- or few-body effects dominate the behavior of the system. At positive scattering length the mixture can for heteronuclear dimers and Bose-condense. In the unitary regime, where the scattering length diverges, stable trimers can form between two layers. On the BCS side of the interspecies Feshbach resonance, two kinds of superfluidity can be observed. For small layer separation d, Cooper pairs can be mediated by the Li atoms interacting with K atoms in two different layers, leading to interlayer s-wave superfluidity. For larger d, intralayer p-wave superfluidity is induced by the interspecies interaction. These four phases are illustrated schematically in Fig. 1.5. Experimentally, such a mixed-dimensionality could be realized by adding a one-dimensional optical lattice that acts only on K with almost

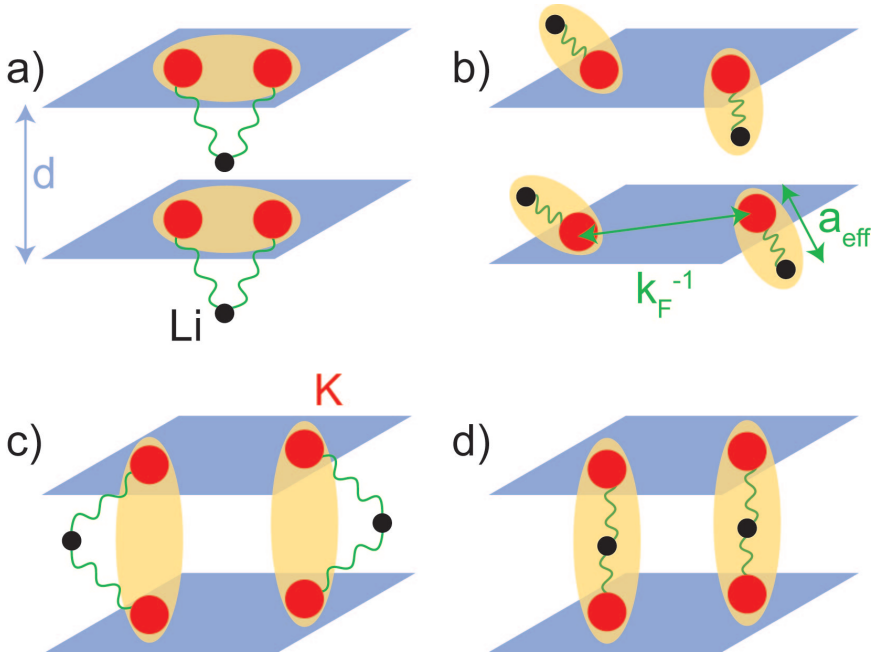

Figure 1.5. Phases of a bilayer Fermi gas at different positions of the phase diagram plotted in Fig. 1.4. Four different situations are illustrated schematically: a) intralayer p-wave superfluidity, b) BEC of dimers, c) mediated interlayer s-wave superfluidity and d) a gas of fermionic trimers.

no effect on the Li. A laser with a relatively small detuning of only a few nm from the K wave length of 767 nm with very low optical power of a few mW would add sufficient confinement on the K in order to be treated as a two-dimensional gas.

The phase diagram of uniform superfluidity for two-species fermion mixtures (^{6}Li and ^{40}K) from the BCS to the BEC limit as a function of scattering parameter and population imbalance is analyzed in Ref. [Isk06]. They find that the zero temperature phase diagram of population imbalance versus scattering parameter is asymmetric for unequal masses, which is in sharp contrast with the symmetric phase diagram for equal masses.

The possibility of a ferroelectric transition in Bose-Bose, Bose-Fermi, or Fermi-Fermi heteronuclear molecules is analyzed in Ref. [Isk07b]. Here they discuss the existence of a ferroelectric Fermi liquid phase for polar Fermi molecules and the existence of a ferroelectric superfluid phase for polar Bose molecules characterized by the coexistence of ferroelectric and superfluid orders and propose an experiment to detect ferroelectric correlations via the observation of coherent dipole radiation pulses.

Similarly to the phase separation in spin-imbalanced mixtures, a Fermi-Fermi mixture yields two stable nonuniform states corresponding to phase separation. In Ref. [Isk08a] phase separation is found between pure unpaired (excess) and pure paired fermions (molecular bosons); and phase separation between pure excess fermions and a mixture of excess fermions and molecular bosons.

The ground state phase diagram of Fermi-Fermi mixtures in optical lattices is

analyzed in Refs. [Isk07a, Isk08b] as a function of interaction strength, fermion filling factor, and tunneling parameters. In addition to standard phases found in homogeneous or harmonically trapped systems, fermions in optical lattices have several insulating phases. These insulating phases include a molecular Bose-Mott insulator (BMI), a Fermi-Pauli (band) insulator (FPI), a phase-separated BMI-FPI mixture or a Bose-Fermi checkerboard (BFC). All these additional phases make the physics of Fermi mixtures much richer than those of atomic bosons or Bose-Fermi mixtures in optical lattices and of harmonically trapped fermions. The molecular BMI phase has been preliminarily observed [Chi06].

Furthermore, the formation of heteronuclear molecules and subsequent transfer to the ground state would create an ultracold gas of molecules with a permanent dipole moment and thus exhibit dipolar interactions. In the case of these heteronuclear molecules the interaction strengths are much larger than for example magnetic rare-earth elements or Rydberg atoms [Lah09].

1.3. Publication Overview

The scope of the present thesis reaches from our first experiments, which determined the basic scattering properties of the ^{6}Li-^{40}K mixture to further studies on the collisional stability of the mixture and on to the creation of a double-degenerate Fermi-Fermi mixture and the observation of heteronuclear molecules. These individual steps have been published in three articles and can be seen as a logical route towards achieving the strongly interacting regime in the mixture. This thesis contains these three published articles, presented in separate Chapters. At the beginning of each article, a short note indicates the primary contribution of this thesis' author to that article.

A detailed description of the experimental setup can be found in the Ph.D. thesis of Eric Wille [Wil09a] in which there is also a more detailed analysis and interpretation of the measurements on interspecies Feshbach resonances presented in Chapter 2. The results published in [Wil08] and the thesis by Eric Wille [Wil09a] established the location of a series of interspecies Feshbach resonances and thus gave first insight into the scattering properties of the ^{6}Li-^{40}K system. Together with our collaborators we could identify various s- and p-wave resonances. Further improvements of the theoretical calculations made it possible to locate resonances which have not yet been observed experimentally. Furthermore, the theoretical models allow to calculate the resonance strengths and widths, thus allowing to identify spin channels with promising prospects for reaching the strongly-interacting regime [Tie10, Tie09].

The next step was to investigate the collisional stability of the three-component Fermi gas of Li in the lowest two spin states together with K in the lowest spin state. These results, published in Ref. [Spi09] are presented in Chapter 3. We report our measurements of the collisional stability of a minority sample of ^{40}K atoms immersed in a bath of ^{6}Li, whose interaction strength can be tuned by means of the broad Feshbach resonance between its two lowest spin states while the interspecies interaction stays constant over the whole range of the Li Feshbach

resonance. Interspecies collisional loss is found to be negligible on the BCS side of the broad Li resonance ($B > 900$ G) and quite weak even exactly on resonance (834 G). Substantial loss, however, occurs on the BEC side of the resonance in a range between about 650 and 800 G. These results allowed us to identify the region of stability of the three-species mixture where we can evaporatively cool Li and sympathetically cool K.

The last publication, presented in Chapter 4, is a longer article [Spi10], which presents the essential experimental steps of our all-optical approach to prepare a double-degenerate Fermi-Fermi mixture of ^{6}Li and ^{40}K atoms, which then serves as a starting point for molecule formation. It describes the optimized trap loading procedures, the internal-state preparation of the sample, and the combined evaporative and sympathetic cooling process. Also discussed is the preparation of the sample near an interspecies Feshbach resonance and we demonstrate the formation of heteronuclear molecules by a magnetic field ramp across the resonance.

1.4. Outlook

Currently, the FeLiKx team is performing precise measurements of the interspecies interaction strength in a Li$|1\rangle$K$|3\rangle$ mixture close to the 155-G Feshbach resonance; see Fig. 4.10 in Section 4.4 for the preparation scheme. A sloshing motion along the trap axis is excited. The resulting oscillation of the Li and K clouds is observed and the damping of the motion is plotted in dependence of the magnetic field as shown in Fig. 1.6. In a simple picture, the damping of the oscillation is directly proportional to the interspecies scattering cross section and we can assume a simple exponential decay of the oscillation amplitude. The advantage of observing collective oscillations is the high precision that can be achieved. This way, we could determine the location of the resonance to be at 154.723 G with an uncertainty of about 5 mG. The width of the resonance is 0.81 G. Also shown in Fig. 1.6 is a fit based on a theoretical calculation of the scattering cross section by Tom Hanna and Paul Julienne from the Joint Quantum Institute at NIST. Adding an offset that accounts for the background damping rate coming from trap inhomogeneities and multiplying with a scaling parameter, the theoretical curve coincides very well with the experimental data.

As can be seen in Fig. 1.6, the damping rate varies over about three orders of magnitude. The maximum value of the scattering length experimentally measured is 656 a_0. Closer to resonance the theoretical model gives scattering lengths of about a factor of 10 larger, which is already big enough for entering the strongly interacting regime. However, the lifetime of the mixture for high scattering rates is on the order of a few ms, much shorter than one oscillation period. This makes it necessary to use a faster oscillatory mode for measuring the scattering length very close to resonance. The radial sloshing mode has a much higher frequency (about a factor of 100 for our trapping geometry) and would thus be well-suited to perform measurements even closer to resonance and possibly even probing the strongly interacting regime. A laser system that allows to species-selectively excite radial oscillations is currently being set up in the laboratory.

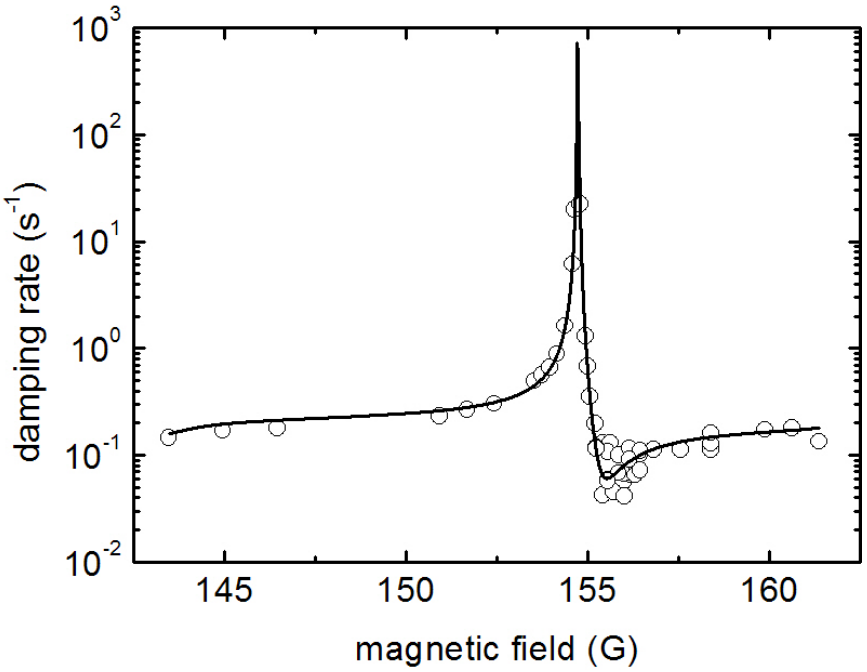

Figure 1.6. Damping of a collective sloshing oscillation of the interspecies Li|1⟩K|3⟩ mixture close to the 155-G Feshbach resonance. Experimental data points are plotted using the open circles. The solid line is a fit based on a coupled-channels calculation of the scattering cross section by Tom Hanna and Paul Julienne.

Observing collective oscillations is a powerful tool to precisely map out interspecies Feshbach resonances. With the implementation of the laser system to excite radial modes the strongly interacting regime is now at reach.

Further steps in the near future include the creation of a heteronuclear molecular BEC and observation of superfluidity in the interspecies mixture for example by observing vortices. Similar to the single-species experiments, the BEC-BCS crossover is an interesting field of study in the interspecies mixtures. However, probing the interspecies crossover will be technically more challenging since the observed Feshbach resonances are very narrow. Furthermore, the implementation of optical lattices could lead to rich and new physics and may lead to improved lifetimes of heteronuclear molecules.

CHAPTER 2

PUBLICATION

Exploring an ultracold Fermi-Fermi mixture: Interspecies Feshbach resonances and scattering properties of ^{6}Li and ^{40}K†

Phys. Rev. Lett. **100**, 053201 (2008)

E. Wille,[1,2] F.M. Spiegelhalder,[1] G. Kerner,[1] D. Naik,[1] A. Trenkwalder,[1]
G. Hendl,[1] F. Schreck,[1] R. Grimm,[1,2] T.G. Tiecke,[3] J.T.M. Walraven,[3]
S.J.J.M.F. Kokkelmans,[4] E. Tiesinga,[5] P.S. Julienne[5]

[1] *Institut für Quantenoptik und Quanteninformation, Österreichische Akademie der Wissenschaften, 6020 Innsbruck, Austria*
[2] *Institut für Experimentalphysik und Zentrum für Quantenphysik, Universität Innsbruck, 6020 Innsbruck, Austria*
[3] *Van der Waals-Zeeman Institute, University of Amsterdam, 1018 XE, The Netherlands*
[4] *Eindhoven University of Technology, P.O. Box 513, 5600 MB Eindhoven, The Netherlands*
[5] *Joint Quantum Institute, National Institute of Standards and Technology and University of Maryland, Gaithersburg, Maryland 20899-8423, USA*

We report on the observation of Feshbach resonances in an ultracold mixture of two fermionic species, ^{6}Li and ^{40}K. The experimental data are interpreted using a simple asymptotic bound state model and full coupled channels calculations. This unambiguously assigns the observed resonances in terms of various s- and p-wave molecular states and fully characterizes the ground-state scattering properties in any combination of spin states.

Fermion pairing and Fermi superfluidity are key phenomena in superconductors, liquid ^{3}He, and other fermionic many-body systems. Our understanding of the underlying mechanisms is far from being complete, in particular for technologically relevant high-T_c superconductors. The emerging field of ultracold atomic Fermi gases

†The primary contribution of the author of the present thesis to this publication is the setup of the K laser system and assisting setting up the electronic control system. He also worked on maintaining and improving the experimental setup.

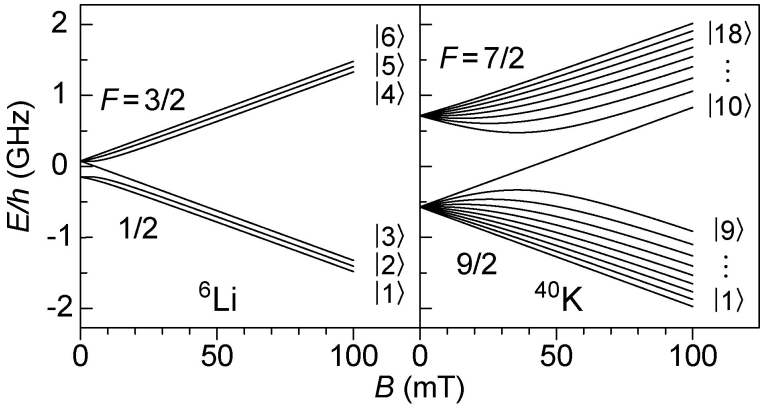

Figure 2.1. Ground state energies of ^{6}Li and ^{40}K versus magnetic field.

has opened up unprecedented possibilities to realize versatile and well-defined model systems. The control of interactions, offered in a unique way by Feshbach resonances in ultracold gases, is a particularly important feature. Such resonances have been used to achieve the formation of bosonic molecules in Fermi gases and to control pairing in many-body regimes [Ing08, Gio08, Chi10, Köh06, Blo08].

So far all experiments on strongly interacting Fermi systems have been based on two-component spin mixtures of the same fermionic species, either ^{6}Li or ^{40}K [Ing08, Gio08]. Control of pairing is achieved via a magnetically tunable *s*-wave interaction between the two states. After a series of experiments on balanced spin mixtures with equal populations of the two states, recent experiments on ^{6}Li have introduced spin imbalance as a new degree of freedom and begun to explore novel superfluid phases [Zwi06, Par06]. Mixing two different fermionic species leads to unprecedented versatility and control. Unequal masses and the different responses to external fields lead to a large parameter space for experiments and promise a great variety of new phenomena [Liu03, Pet05, Isk06, Ors08, Pet07]. The combination of the two fermionic alkali species, ^{6}Li and ^{40}K, is a prime candidate to realize strongly interacting Fermi-Fermi systems.

In this Letter, we realize a mixture of ^{6}Li and ^{40}K and identify heteronuclear Feshbach resonances [Sta04, Ino04, Fer06a, Fer06b]. This allows us to characterize the basic interaction properties. Figure 2.1 shows the atomic ground-state energy structure. We label the energy levels Li$|i\rangle$ and K$|j\rangle$, counting the states with rising energy. The hyperfine splitting of ^{6}Li is $(3/2)a_{\rm hf}^{\rm Li}/h = 228.2\,$MHz. For ^{40}K, the hyperfine structure is inverted and the splitting amounts to $(9/2)a_{\rm hf}^{\rm K}/h = -1285.8\,$MHz [Ari77]. For the low-lying states with $i \le 3$ and $j \le 10$, the projection quantum numbers are given by $m_{\rm Li} = -i + 3/2$ and $m_{\rm K} = j - 11/2$. A Li$|i\rangle$K$|j\rangle$ mixture can undergo rapid decay via spin relaxation if exoergic two-body processes exist that preserve the total projection quantum number $M_{\rm F} = m_{\rm Li} + m_{\rm K} = -i + j - 4$. Whenever one of the species is in the absolute ground state and the other one is in a low-lying state ($i = 1$ and $j \le 10$ or $j = 1$ and $i \le 3$), spin relaxation is strongly suppressed [Sim03].

We prepare the mixture in an optical dipole trap, which is formed by two 70 W-laser beams (wavelength 1070 nm), crossing at an angle of 12° [Spi10]. The dipole

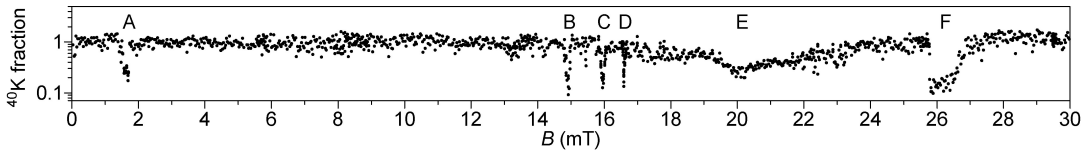

Figure 2.2. Feshbach scan of the Li|1⟩K|2⟩ mixture. The remaining fraction of ^{40}K atoms relative to off-resonant regions after 10 s interaction with ^{6}Li atoms is shown as a function of magnetic field. Loss features A, B, C, D, and F are due to interspecies Feshbach resonances. Loss feature E is caused by a ^{40}K p-wave Feshbach resonance [Reg03b].

trap is loaded with about 10^7 ^{6}Li atoms and a few 10^4 ^{40}K atoms from a two-species magneto-optical trap (MOT). At this stage the trap depth for ^{6}Li (^{40}K) is 1.7 mK (3.6 mK) and the trap oscillation frequencies are 13 kHz (7.3 kHz) and 1.7 kHz (1.0 kHz) in radial and axial directions. After preparation of the internal states of the atoms [Spi10], a balanced mixture of Li|1⟩ and Li|2⟩ atoms together with K|1⟩ atoms is obtained. We perform evaporative cooling at a magnetic field of 76 mT close to the 83.4 mT Feshbach resonance between Li|1⟩ and Li|2⟩ [Ing08, Gio08] by reducing the optical dipole trap depth exponentially by a factor of 70 over 2.5 s. We observe that potassium remains thermalized with lithium during the evaporation. This results in 10^5 Li|1⟩ and 10^5 Li|2⟩ atoms together with 10^4 K|1⟩ atoms at a temperature of 4 μK. This three-component Fermi mixture serves as a starting point to prepare several different stable two-component mixtures, namely Li|2⟩K|1⟩, Li|1⟩K|1⟩, Li|1⟩K|2⟩, or Li|1⟩K|3⟩ with $M_F = -5, -4, -3, -2$, respectively. Atoms in the K|1⟩ state are transferred to the desired state with adiabatic radio-frequency sweeps. Population in unwanted states is pushed out of the trap by pulses of resonant light [Spi10]. Finally, to increase the collision rate, the sample is compressed by increasing the power of the optical trap. The temperature rises to 12 μK and the peak density of lithium (potassium) increases to about 10^{12}cm^{-3} (few 10^{11}cm^{-3}).

We detect Feshbach resonances by observing enhanced atom loss at specific values of the magnetic field [Chi10], which is caused by three-body decay. For each mixture we perform a magnetic field scan with a resolution of 0.03 mT between 0 and 74 mT (0 to 40 mT for the Li|1⟩K|3⟩ mixture). A scan consists of many experimental cycles, each with a total duration of about one minute during which the mixture is submitted for ten seconds to a specific magnetic field value. The quantity of remaining atoms is measured by recapturing the atoms into the MOTs and recording their fluorescence light.

In Fig. 2.2, we show a loss spectrum of Li|1⟩K|2⟩. A striking feature is that the potassium atom number decreases by an order of magnitude at specific values of the magnetic field. Since the mixture contains an order of magnitude more lithium than potassium atoms, the lithium atom number does not change significantly by interspecies inelastic processes. Therefore, the potassium loss is exponential and near complete. In order to distinguish loss mechanisms involving only one species from those involving two species, we perform additional loss measurements, using samples of either pure ^{6}Li or pure ^{40}K. Loss features A, B, C, D, and F only appear using a two-species mixture. Loss feature E persists in a pure ^{40}K sample and can

be attributed to a potassium p-wave Feshbach resonance [Reg03b]. On the basis of the experimental data only, we can not unambiguously attribute loss feature C to an interspecies Feshbach resonance, since it coincides with a known ^{6}Li p-wave resonance [Zha04, Sch05].

Our main findings on positions and widths ΔB of the observed loss features are summarized in Table 2.1, together with the results of two theoretical models described in the following.

Our analysis of the data requires finding the solutions for the Hamiltonian $H = H_\alpha^{\rm hf} + H_\beta^{\rm hf} + H^{\rm rel}$. To underline the generality of our model, we refer to Li as α and to K as β. The first two terms represent the hyperfine and Zeeman energies of each atom, $H^{\rm hf} = (a_{\rm hf}/\hbar^2)\mathbf{s}\cdot\mathbf{i} + \gamma_e\mathbf{s}\cdot\mathbf{B} - \gamma_n\mathbf{i}\cdot\mathbf{B}$, where $\mathbf{s}$ and $\mathbf{i}$ are the single-atom electron and nuclear spin, respectively, and γ_e and γ_n are the respective gyromagnetic ratios. The Hamiltonian of relative motion is

$$H^{\rm rel} = \frac{\hbar^2}{2\mu}\left(-\frac{d^2}{dr^2} + \frac{l(l+1)}{r^2}\right) + \sum_{S=0,1} V_S(r)P_S, \tag{2.1}$$

where μ is the reduced mass, r is the interatomic separation, and l is the angular momentum quantum number for the relative motion. Defining the total electron spin as $\mathbf{S} = \mathbf{s}_\alpha + \mathbf{s}_\beta$, the projection operator P_S either projects onto the $S = 0$ singlet or $S = 1$ triplet spin states. The potential $V_S(r)$ is thus either for the singlet $X^1\Sigma$ or triplet $a^3\Sigma$ state. This Hamiltonian H conserves both l and $M_{\rm F}$.

Our first method to locate the Feshbach resonances is inspired by a two-body bound state model for homonuclear [Moe95] and heteronuclear [Sta04] systems. We have expanded this previous work to include the part of the hyperfine interaction that mixes singlet and triplet levels. This mixing is crucial for the present analysis. We refer to this model as the Asymptotic Bound state Model (ABM).

The ABM model expands the bound state solutions $|\Psi^l\rangle$ for each l in terms of $|\psi_S^l\rangle|S, M_S, \mu_\alpha, \mu_\beta\rangle$ where $|\psi_S^l\rangle$ is the asymptotic last bound eigenstate of the potential $V_S(r) + \hbar^2 l(l+1)/(2\mu r^2)$ and $|S, M_S, \mu_\alpha, \mu_\beta\rangle$ are spin functions where M_S, μ_α and μ_β are the magnetic quantum numbers of $\mathbf{S}$, $\mathbf{i}_\alpha$ and $\mathbf{i}_\beta$, respectively. Only spin functions with the same conserved $M_{\rm F} = M_S + \mu_\alpha + \mu_\beta$ are allowed. Note that $S, M_S, \mu_\alpha, \mu_\beta$ are good quantum numbers for large magnetic field. Expanding $|\Psi^l\rangle$ in this basis and assuming that the overlap $\langle\psi_0^l|\psi_1^l\rangle$ is unity [1], the coupled bound state energies are found by diagonalizing the interaction matrix [Spi10].

The energies E_S^l of the last bound state of the $S = 0$ and 1 potentials are eigenvalues of Eq. (2.1), and serve as free parameters in the ABM model. We can reduce this to only two binding energy parameters $E_0 = -E_0^0$ and $E_1 = -E_1^0$ if we use information about the actual shape of the potential. We can do this using model potentials derived from Refs. [Sal07] and [Aym05], and the van der Waals coefficient $C_6 = 2322\,E_{\rm h}\,a_0^6$ ($E_{\rm h} = 4.35974 \times 10^{-18}$ J and $a_0 = 0.0529177$ nm) [Der01]. Each E_S can be varied by making small changes to the short range potential while keeping C_6 fixed. The energy E_S uniquely determines both the s-wave scattering length as well as E_S^l for $l > 0$.

[1] The actual values are 0.979 for $l = 0$ and 0.965 for $l = 1$.

Table 2.1. Feshbach resonances in collisions between ^{6}Li and ^{40}K in a range from 0 to 76 mT. For their positions B_0, we give the center of the measured loss features and the results from both the ABM and coupled channels calculations. The first columns give the ^{6}Li and ^{40}K channel indices i and j and the projection quantum number $M_F = -i + j - 4$. Note that the experimental width of a loss feature, ΔB, is not the same thing as the width ΔB_s related to the scattering length singularity. The latter is only defined for s-wave resonances, and not for the observed p-wave resonances. The typical statistical and systematic error in the experimental B_0 is about 0.05 mT for s-wave resonances.

		Experiment		ABM	Coupled channels	
i, j	M_F	B_0 (mT)	ΔB (mT)	B_0 (mT)	B_0 (mT)	ΔB_s (mT)
2, 1	-5	21.56[a]	0.17	21.67	21.56	0.025
1, 1	-4	15.76	0.17	15.84	15.82	0.015
1, 1	-4	16.82	0.12	16.92	16.82	0.010
1, 1	-4	24.9	1.1	24.43	24.95	p wave
1, 2	-3	1.61	0.38	1.39	1.05	p wave
1, 2	-3	14.92	0.12	14.97	15.02	0.028
1, 2	-3	15.95[a]	0.17	15.95	15.96	0.045
1, 2	-3	16.59	0.06	16.68	16.59	0.0001
1, 2	-3	26.3	1.1	26.07	26.20	p wave
1, 3	-2	not observed		1.75	1.35	p wave
1, 3	-2	14.17	0.14	14.25	14.30	0.036
1, 3	-2	15.49	0.20	15.46	15.51	0.081
1, 3	-2	16.27	0.17	16.33	16.29	0.060
1, 3	-2	27.1	1.4	27.40	27.15	p wave

Figure 2.3 shows the bound state energies of the ABM model as a function of magnetic field for $M_F = -3$. Feshbach resonances occur at the crossings of bound states and threshold. We find a good fit for the experimental resonance positions for parameters E_0/h = 716(15) MHz and E_1/h=425(5) MHz, where the uncertainty represents one standard deviation, see Table 2.1.

For additional analysis we have also used exact, yet much more computationally complex coupled channels calculations [Sto88], varying the short range potential as discussed above. An optimized fit to the measured resonance positions gives E_0/h=721(10) MHz and E_1/h = 426(3) MHz. This corresponds to a singlet scattering length of 52.1(3) a_0 and a triplet scattering length of 63.5(1) a_0. Thus, within the fitting accuracy to the experimental data, the prediction of the ABM model agrees with the result of the full coupled channels calculation. Table 2.1 shows the coupled channels resonance locations and widths for a representative calculation with E_0/h = 720.76 MHz and E_1/h = 427.44 MHz. The s-wave resonance width ΔB_s is defined by $a_s(B) = a_{bg}(1 - \Delta B_s/(B - B_0))$, where a_{bg} is the background scattering length near the resonance position B_0. Note that ΔB_s need not be the same as the empirical width ΔB of a loss-feature. All resonances except the $M_F = -3$ p-wave resonance

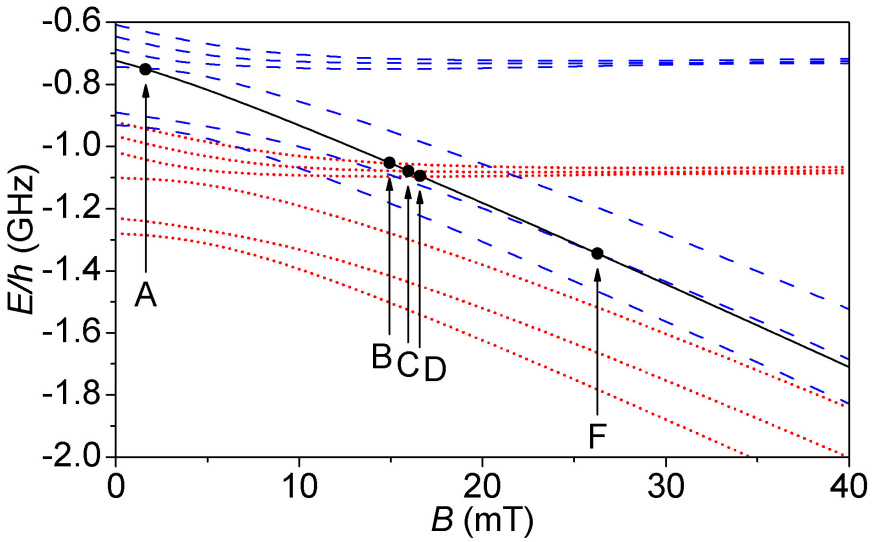

Figure 2.3. Bound state energies versus magnetic field. Dotted (dashed) lines indicate the s-wave (p-wave) states. The two-body threshold for the Li$|1\rangle$K$|2\rangle$ collision channel ($M_F = -3$) is indicated by the solid line. The dots and the corresponding arrows indicate the measured resonance positions (see Fig. 2.2).

near 1.6 mT agree with the measured positions within 0.13 mT. Fine-tuning of the long range potential would be needed to fit this resonance to comparable accuracy. Figure 2.4 shows the calculated s-wave scattering lengths and p-wave elastic cross sections versus magnetic field B for this model. The background scattering length a_{bg} for the s-wave resonances is approximately 63 a_0.

The accuracy and computational simplicity of the ABM model make resonance assignments very efficient, allowing rapid feedback between the experiment and theory during the exploratory search for resonances. As the ABM model in its present form does not yield the width of the resonances, the prediction of a resonance position is not expected to be more accurate than the corresponding experimental resonance width. For the ^{6}Li-^{40}K mixture, the ABM model predicts hundreds of further resonances in various s- and p-wave channels up to 0.1 T [Spi10].

A remarkable feature of the ^{6}Li-^{40}K system is the large widths of the p-wave resonances near 25 mT, which by far exceeds the width of the observed s-wave resonances. Naively, one would expect the s-wave resonances to be wider than their p-wave counterparts because of the different threshold behavior. However, in the present case the difference in magnetic moments between the atomic threshold and the relevant molecular state is found to be anomalously small, which stretches out the thermally broadened p-wave resonance features over an unusually wide magnetic field range. Also the asymmetry of the loss feature supports its interpretation as a p-wave resonance [Zha04, Sch05, Che05b].

An important issue for future experiments is the character of the s-wave resonances, i.e. the question whether they are entrance-channel or closed-channel dominated [Chi10, Köh06]. All our observed resonances are rather narrow and

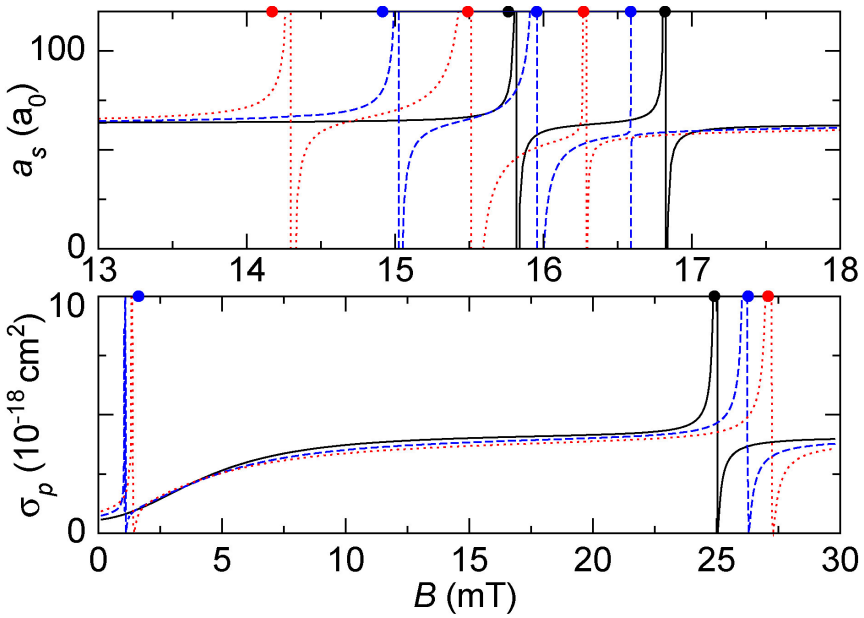

Figure 2.4. Results from coupled channels calculations for the magnetic-field dependence of the s-wave scattering length $a_s(B)$ (upper panel) and the $m_l = 0$ contribution to the p-wave elastic scattering cross section $\sigma_p(E)$ for $E/k_B = 12\,\mu$K (lower panel) for the channels in Table 2.1 with $M_F = -4$ (solid line), -3 (dashed line), and -2 (dotted line). The dots indicate the measured resonance locations.

thus closed-channel dominated. The existence of entrance-channel dominated resonances would be of great interest to experimentally explore BEC-BCS crossover physics [Ing08, Gio08] in mixed Fermi systems. However, our coupled channels calculations for a partial set of predicted resonances have not yet found any such resonances, and their existence seems unlikely in view of the moderate values of the background scattering lengths [Chi10, Köh06].

In conclusion, we have characterized the interaction properties in an ultracold mixture of ^{6}Li and ^{40}K atoms by means of Feshbach spectroscopy and two theoretical models. The results are of fundamental importance for all further experiments in the emerging field of Fermi-Fermi mixtures. Further steps will be the formation of bosonic ^{6}Li^{40}K molecules through a Feshbach resonance and evaporative cooling towards the creation of a heteronuclear molecular Bose-Einstein condensate.

A double-degenerate mixture of ^{6}Li and ^{40}K was recently demonstrated in a magnetic trap [Tag08].

We thank E. Tiemann for stimulating discussions. The Innsbruck team acknowledges support by the Austrian Science Fund (FWF) and the European Science Foundation (ESF) within the EuroQUAM project. TGT and JTMW acknowledge support by the FOM-Program for Quantum gases. SJJMFK acknowledges support from the Netherlands Organization for Scientific Research (NWO). PSJ acknowledges partial support by the U.S. Office of Naval Research.

CHAPTER 3

PUBLICATION

Collisional Stability of ^{40}K Immersed in a Strongly Interacting Fermi Gas of ^{6}Li[†]

Phys. Rev. Lett. **103**, 223203 (2009)

F.M. Spiegelhalder,[1] A. Trenkwalder,[1] D. Naik,[1] G. Hendl,[1] F. Schreck,[1] R. Grimm,[1,2]

[1] *Institut für Quantenoptik und Quanteninformation, Österreichische Akademie der Wissenschaften, 6020 Innsbruck, Austria*
[2] *Institut für Experimentalphysik und Zentrum für Quantenphysik, Universität Innsbruck, 6020 Innsbruck, Austria*

We investigate the collisional stability of a sample of ^{40}K atoms immersed in a tunable spin mixture of ^{6}Li atoms. In this three-component Fermi-Fermi mixture, we find very low loss rates in a wide range of interactions as long as molecule formation of ^{6}Li is avoided. The stable fermionic mixture with two resonantly interacting spin states of one species together with another species is a promising system for a broad variety of phenomena in few- and many-body quantum physics.

The groundbreaking achievements in experiments with ultracold Fermi gases have opened up unprecedented possibilities to study new regimes of strongly interacting quantum matter [Ing08, Gio08, Blo08]. Recent experiments have opened up two important new research frontiers with fermionic atoms that go beyond the two-component spin mixtures so far exploited in the field. Mixtures involving three different spin states [Ott08, Huc09] and mixtures of different fermionic species [Tag08, Wil08, Tie10] have produced first exciting results like the demonstration of fermionic Efimov states [Wen09, Wil09b] and the creation of Fermi-Fermi molecules [Voi09, Spi10].

[†]The author of the present thesis performed all the measurements in this publication and contributed to the setup of the optical dipole traps. He also setup the new Li diode laser system and implemented high-field imaging of Li and K at 1190 G. The main part of the data analysis for this publication was done by A.T. and D.N.

A key ingredient in the success story of strongly interacting Fermi gases is their collisional stability. In contrast to other systems with large scattering lengths, which usually exhibit very fast collisional decay, a two-component Fermi gas can be extraordinarily stable. This results from Pauli suppression effects in atomic three-body decay [Esr01] and in atom-dimer and dimer-dimer collisions [Pet04]. Obviously, such a suppression effect is absent when three distinguishable particles interact. This raises general questions concerning collisionally stable regimes and thus the possibilities for experiments on multicomponent Fermi gases with strong interactions. The recent experiments [Ott08, Huc09] on three-component spin mixtures of ^{6}Li have indeed shown very rapid collisional decay in regimes involving large scattering lengths.

In this Letter, we experimentally explore a three-component Fermi gas with strong interactions between two of its components. A single spin state of ^{40}K is immersed in a deeply degenerate two-component spin mixture of ^{6}Li atoms. While the intraspecies interaction between the two ^{6}Li spin states can be tuned to arbitrarily large strength, the interspecies interaction remains weak. We find that a wide stable region exists where elastic collisions dominate over inelastic decay. This opens up a variety of new exciting experimental possibilities. Here we demonstrate two immediate applications, the sympathetic cooling of another species by a strongly interacting Fermi gas and the possibility of precise thermometry in the strongly interacting regime.

The Fermi-Fermi mixture is prepared in an optical dipole trap [Spi10]. Initially about 10^7 Li atoms and a few 10^4 K atoms are loaded from a two-species magneto-optical trap (MOT) into the focus of an intense infrared laser beam (initial power 70 W, wavelength 1070 nm, waist 25 μm). The spin states are prepared such that Li is in an equal mixture of its two lowest energy states, labeled Li$|1\rangle$ and Li$|2\rangle$, and K is in its lowest state, labeled K$|1\rangle$. After a forced evaporative cooling process, which takes typically 10 s, the atoms are trapped in a 75 mW beam (waist ~45μm). In the final evaporation phase, the axial trapping is essentially provided by the magnetic-field curvature of 28 G/cm^2 [Joc03]. Throughout the whole evaporation process the magnetic field is set to 1190 G, above the broad 834-G Feshbach resonance [Ing08, Gio08], where the scattering length between the two ^{6}Li spin states is $a = -2900\,a_0$ (a_0 is Bohr's radius). Finally, to avoid further evaporative loss, the sample is recompressed by a twofold increase of the trap depth [1]. We obtain a mixture of about 10^5 Li atoms per spin state at a temperature $T^{\mathrm{Li}} \approx 100$ nK together with about 4×10^3 K atoms at a temperature $T^{\mathrm{K}} \approx 140$ nK; note that the two species are not fully thermalized at this point, such that $T^{\mathrm{K}} > T^{\mathrm{Li}}$. In terms of the corresponding Fermi temperatures $T_F^{\mathrm{Li}} = 650$ nK and $T_F^{\mathrm{K}} = 90$ nK, the temperatures can be expressed as $T^{\mathrm{Li}}/T_F^{\mathrm{Li}} \approx 0.15$ and $T^{\mathrm{K}}/T_F^{\mathrm{K}} \approx 1.6$.

This ultracold mixture serves as the starting point for our investigation of collisional loss throughout the crossover of the ^{6}Li gas from molecular Bose-Einstein condensation (BEC) to Bardeen-Cooper-Schrieffer (BCS) type behavior [Ing08, Gio08, Blo08]. This BEC-BCS crossover is controlled by the magnetic field via the broad ^{6}Li

[1] The oscillation frequencies for Li (K) are 26 Hz (10 Hz) axially, and 450 Hz (260 Hz) radially, and the trap depth is 3 μK (6 μK).

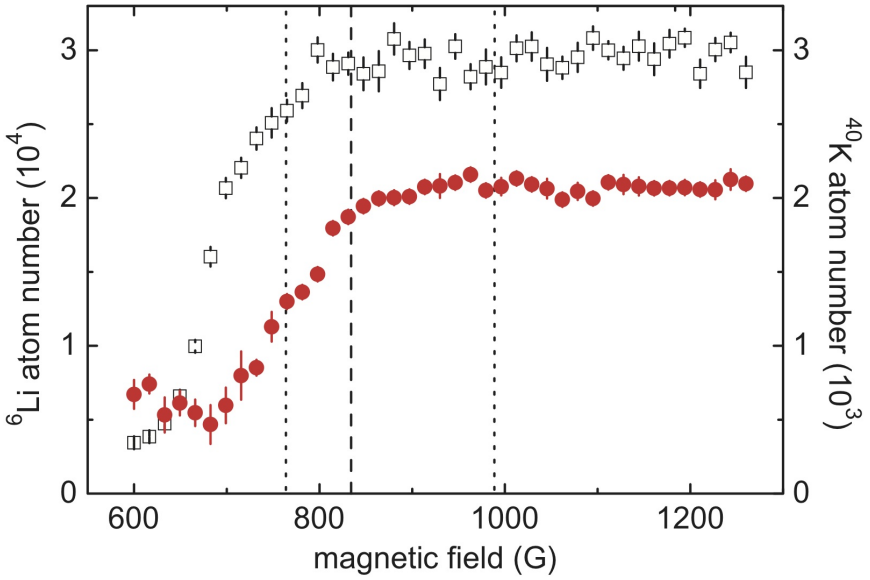

Figure 3.1. Remaining number of ^{6}Li atoms per spin state (open squares) and of ^{40}K atoms (filled circles) after a hold time of 1 s at a variable magnetic field. The dashed line at 834 G marks the center of the broad ^{6}Li Feshbach resonance and the dotted lines at 765 and 990 G indicate the strongly interacting regime, where $|k_F^{\mathrm{Li}} a| \geq 1$. The error bars indicate the statistical error of ten measurements.

Feshbach resonance centered at 834 G. Under our conditions, with a Li Fermi wave number $k_F^{\mathrm{Li}} = 1/(4400\, a_0)$, the strongly interacting regime ($|k_F^{\mathrm{Li}} a| \geq 1$) is realized between 765 and 990 G. Note that there are no interspecies Feshbach resonances in the corresponding magnetic field range and the interspecies scattering length remains constantly small at about $+60\, a_0$ [Wil08]. Since there are typically 25 times less K atoms in the trap than Li atoms, the Li sample remains essentially unperturbed by K.

In a first set of experiments, we ramp the magnetic field to a variable value and study the loss of atoms during a 1-s hold time. For detection, the remaining atoms are recaptured into the two-species MOT and their fluorescence is recorded. The atom numbers determined from fluorescence are calibrated by absorption images.

The loss of Li and K atoms around the 834-G Li Feshbach resonance is shown in Fig. 3.1. The Li sample, essentially unperturbed by K, shows a pattern observed previously [Die02, Bou03, Joc04]. On the BCS side of the resonance (≥ 834 G), Li loss is very small and the detected signal stays nearly constant. On the BEC side, the observed loss results from the vibrational relaxation of dimers during dimer-dimer and atom-dimer collisions [Pet04]. The K signal shows a very similar behavior. While loss is very weak on the BCS side of the Li resonance, strong loss is observed on the BEC side with a maximum around 700 G. At even lower fields, where Li decays very quickly, more K atoms are found to remain. This observation already points to the fact that the main source of K loss results from collisions with Li dimers.

In a second set of experiments, we study the loss more quantitatively and record the time evolution of the atom numbers for several magnetic field values. Example

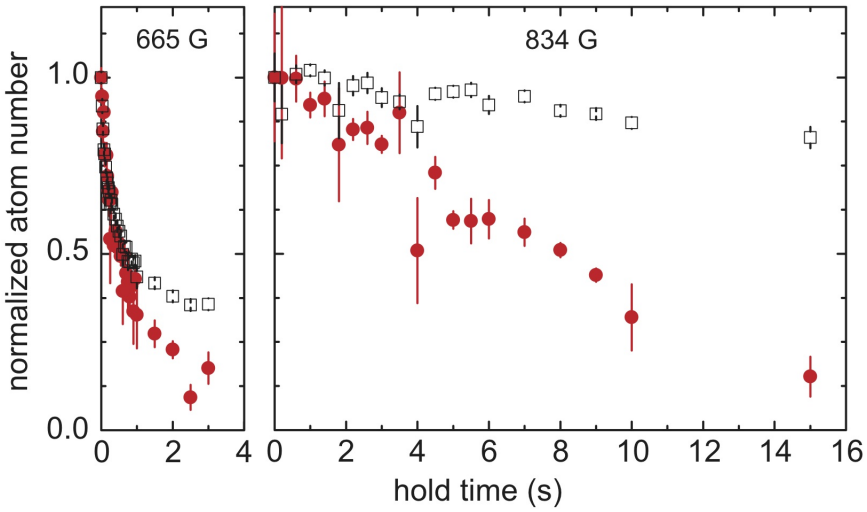

Figure 3.2. ^{6}Li (open squares) and ^{40}K (filled circles) atom number normalized to the respective initial atom number over hold time for 665 G and 834 G.

decay curves are shown in Fig. 3.2. We describe K loss by the rate equation $\dot{N}_K/N_K = -\Gamma_{bg} - L_2\langle n_{Li}\rangle - L_3\langle n_{Li}^2\rangle$, where the angle brackets denote averages weighted by the K density distribution. N_K is the K atom number, n_{Li} the density distribution of a single Li state and Γ_{bg} the background loss rate. The coefficient L_2 describes two-body loss resulting from inelastic collisions of K atoms with Li dimers. The coefficient L_3 takes into account three-body loss that results from collisions of a K atom with two Li atoms in different spin states. Both loss processes involve three distinguishable atoms, for which there is no Pauli suppression effect as in two-component Fermi systems [Esr01, Pet04].

For short decay times, the Li density and the K temperature do not change significantly and $-\dot{N}_K/N_K$ corresponds to an initial decay rate Γ. We determine Γ as the initial slope of an exponential fit to the first 0.5 s of K decay data (0.3 s for the 665 G data point). K and Li density distributions are calculated from measured atom numbers, temperatures, and trap oscillation frequencies [2]. From unitarity to the BCS region, the K cloud is small compared to the Li cloud and essentially probes the center of the Li sample. On resonance, where the peak Li density is $n_{Li,peak} = 2.1\times10^{12}$ cm^{-3} for each spin state, we find $n_{Li,peak}/\langle n_{Li}\rangle = 1.7$ and $n_{Li,peak}^2/\langle n_{Li}^2\rangle = 2.4$. For the data point at the lowest magnetic field (665 G) the Li sample shrinks [Bar04] to a size smaller than the K sample and it becomes important to consider the averaged Li density, illustrated by the fact that $n_{Li,peak}/\langle n_{Li}\rangle = 4$ and $n_{Li,peak}^2/\langle n_{Li}^2\rangle = 6.7$.

Based on our experimental data alone we cannot distinguish between two-body or three-body loss processes. We therefore analyze the data by fully attributing the loss to either one of these two processes, after subtracting the measured background loss. This results in coefficients $\mathscr{L}_2 = (\Gamma-\Gamma_{bg})/\langle n_{Li}\rangle$ and $\mathscr{L}_3 = (\Gamma-\Gamma_{bg})/\langle n_{Li}^2\rangle$, which in general represent upper limits for the real loss coefficients L_2 and L_3. The

[2] The K density distribution is approximated as Gaussian. The Li distribution is approximated by a $T = 0$ Fermi distribution, rescaled in dependence of the magnetic field.

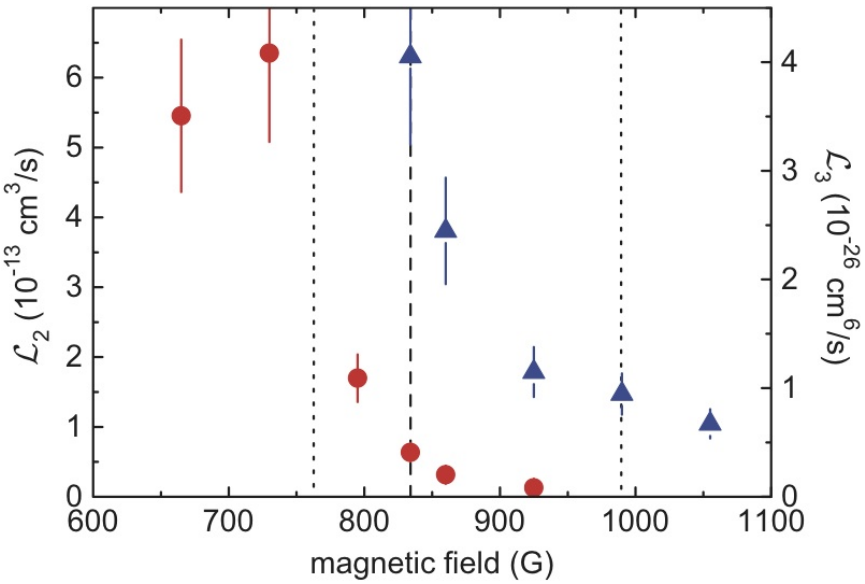

Figure 3.3. Upper bounds $\mathscr{L}_2$ and $\mathscr{L}_3$ (circles and triangles, respectively) for the two- and three body loss rate coefficients of ^{40}K immersed in a strongly interacting degenerate ^{6}Li sample throughout the ^{6}Li BEC-BCS crossover. The dashed line at 834 G marks the center of the broad ^{6}Li Feshbach resonance and the dotted lines at 765 and 990 G indicate the strongly interacting regime, where $|k_F^{\mathrm{Li}} a| \geq 1$. The error bars represent the statistical errors from fitting the loss curves. Additional uncertainties arise from our limited knowledge of the size of the Li sample. On the BCS side this is negligible in comparison with the shown statistical errors, but on the BEC side it may introduce additional errors of up to a few 10%.

background loss rate Γ_{bg}=0.009 s^{-1} is determined by analyzing the decay of a pure K sample. Above fields of 900 G the interspecies loss rate is comparable to this background loss rate.

The upper bounds $\mathscr{L}_2$ and $\mathscr{L}_3$ for the loss coefficients are shown in Fig. 3.3. They peak around 730 G and decrease by more than an order of magnitude for fields of 925 G and above. We expect the dominant loss process to change within the ^{6}Li BEC-BCS crossover. Far on the BEC side, virtually all Li atoms are bound in Li_2 molecules. Potassium is expected to be lost mainly as a result of inelastic two-body collisions with those molecules. At 665 G the real loss rate coefficient L_2 is therefore expected to be very close to $\mathscr{L}_2$, for which we obtain a value of about 6×10^{-13} cm^{-3}/s. Closer to resonance on the BEC side, atom-dimer loss is substantially reduced in accordance with the predictions of Ref. [D'I08]. Far on the BCS side, no Li dimers exist and three-body recombination involving a K$|1\rangle$, a Li$|1\rangle$, and a Li$|2\rangle$ atom can be expected to be the dominant interspecies loss process. At 1190 G L_3 is therefore expected to be very close to $\mathscr{L}_3$, for which we obtain a value of 0.7×10^{-26} cm^{-6}/s. Near the Feshbach resonance, in the strongly interacting regime, the interpretation of loss is not as straightforward. Three-body loss and an effective two-body loss resulting from collisions with Li pairs may both contribute [Du09]. At the resonance center (834G) we find $\mathscr{L}_2 = 0.6 \times 10^{-13}$ cm^{-3}/s and $\mathscr{L}_3 = 4 \times 10^{-26}$ cm^{-6}/s.

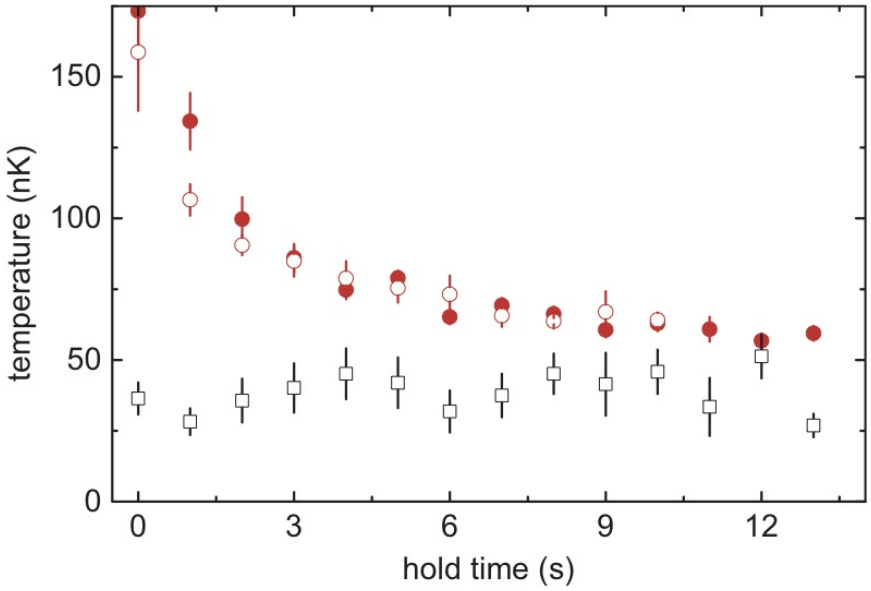

Figure 3.4. Thermalization of ^{40}K in a ^{6}Li bath. The temperature evolution of the ^{40}K probe is shown at 1190 G (filled circles) and at 834 G (open circles). For comparison we also show the temperature of the ^{6}Li bath measured at 1190 G. The error bars represent the fit errors from analyzing time-of-flight images.

Deeper cooling of the Fermi-Fermi mixture leads into the double-degenerate regime [Spi10]. This is achieved by a simple extension of the evaporative cooling process. After completing the forced evaporation ramp (stage I), we hold the sample in the shallow trap for up to 13 s (stage II) [3]; here the Fermi energies are $T_F^{\mathrm{Li}} = 420\,\mathrm{nK}$ and $T_F^{\mathrm{K}} = 95\,\mathrm{nK}$. In this situation, the Li bath undergoes continuous plain evaporation, which can efficiently remove any heat deposited by the K sample or caused by residual heating processes. Initially the bath of Li atoms contains 3.9×10^4 per spin state and losses throughout stage II remain below 20%. The temperature of the Li bath, as determined by fitting Fermi distributions to absorption images of the cloud after trap release, stays constantly at $T^{\mathrm{Li}} \approx 40\,\mathrm{nK}$.

Figure 3.4 shows how the K component is cooled down sympathetically into the quantum-degenerate regime. The temperature T^{K} is measured by standard time-of-flight absorption imaging. After the evaporation ramp T^{K} starts at about 170 nK, as the ramp in stage I is too fast to establish an interspecies thermal equilibrium. In stage II, with the magnetic field kept at 1190 G (filled circles), the temperature of the 3.4×10^3 K atoms slowly approaches a final value of ~60 nK, corresponding to $T^{\mathrm{K}}/T_F^{\mathrm{K}} = 0.6$. From an exponential fit to T^{K}, we derive a $1/e$ time constant for the sympathetic cooling process of ~3 s. For the Li-K mass ratio, thermalization requires about six collisions [Mud02], giving ~2 s^{-1} for the elastic collision rate. For comparison, we also study the sympathetic cooling when the magnetic field in stage II is set to 834 G. In this case, the Li bath forms a strongly interacting superfluid with

[3] In stage II, the trap oscillation frequencies for Li (K) are 26 Hz (10 Hz) axially, and 330 Hz (190 Hz) radially. The trap depth is 1.5 μK (3 μK)

unitarity-limited interactions [Ing08, Gio08]. The only difference observed for the two settings of the magnetic field in stage II is a loss of about 40% of the K atoms at 834 G in contrast to an essentially lossless situation at 1190 G.

Our data in Fig. 3.4 indicate that the final K temperature stays somewhat above the temperature of the Li bath. This could be readily explained by the presence of a weak heating process of about 5 nK/s for K counteracting the sympathetic cooling. Another possible explanation could be that we underestimate the Li temperature because of systematic problems with thermometry of deeply degenerate Fermi gases, in particular in our shallow trap with considerable anharmonicities. The final temperatures reached in the sympathetic cooling process need further investigations. In any case, the measurement of the K temperature is free from such systematic errors and thus provides a firm upper bound for the true temperature of the Li bath. Also, a comparison of the scatter and error bars of the data in Fig. 3.4 for both species highlights that the K thermometry is much less affected by statistical errors, though performed with an order of magnitude less atoms. These observations point to the great potential of a weakly interacting probe species for precise thermometry in strongly interacting Fermi gases, which in generally is a very difficult task [Ing08, Luo09, Shi08]. Note that an impurity thermometer relying on basically the same idea was demonstrated for a Fermi gas of ^{40}K atoms in Ref. [Reg05a], using a third spin state instead of another species. For stability reasons, however, it was not applied in the strongly interacting regime.

Our ultracold ^{40}K-^{6}Li combination demonstrates the experimental possibility to immerse another species in a strongly interacting Fermi gas without suffering from collisional loss. With the examples of sympathetic cooling and thermometry we have shown two straightforward applications. There are many more experimental options with the potential to break new ground in research with ultracold fermions. The immersed species can in general serve as a weakly interacting probe for the fermionic superfluid with the great advantages that it can be separately addressed, manipulated, and detected by laser and radio-frequency fields. This may be exploited to study interactions in the many-body regime such as atom-pair collisions or to test the viscosity or the superfluid behavior of the system by a controlled motion of the impurity. Moreover, our double-degenerate system represents an excellent starting point to study a rich variety of phenomena related to few-body quantum states [Pet05, Nis09b, Lev09] and the rich many-body quantum phases of multicomponent Fermi mixtures [Paa06, Isk06, Isk07a, Pet07, Isk08c, Bar08, Bau09, Nis09a, Wan09, Mor09].

We acknowledge support by the Austrian Science Fund (FWF) and the European Science Foundation (ESF) within the EuroQUAM/FerMix project and support by the FWF through the SFB FoQuS.

CHAPTER 4

PUBLICATION

All-optical production of a degenerate mixture of ^{6}Li and ^{40}K and creation of heteronuclear molecules[†]

Phys. Rev. A submitted (2010)

F.M. Spiegelhalder,[1] A. Trenkwalder,[1] D. Naik,[1] G. Kerner,[1]
E. Wille,[1,2,*] G. Hendl,[1] F. Schreck,[1] R. Grimm,[1,2]

[1] *Institut für Quantenoptik und Quanteninformation, Österreichische Akademie der Wissenschaften, 6020 Innsbruck, Austria*
[2] *Institut für Experimentalphysik und Zentrum für Quantenphysik, Universität Innsbruck, 6020 Innsbruck, Austria*
[*] *Current address: European Space Agency, Noordwijk, The Netherlands*

We present the essential experimental steps of our all-optical approach to prepare a double-degenerate Fermi-Fermi mixture of ^{6}Li and ^{40}K atoms, which then serves as a starting point for molecule formation. We first describe the optimized trap loading procedures, the internal-state preparation of the sample, and the combined evaporative and sympathetic cooling process. We then discuss the preparation of the sample near an interspecies Feshbach resonance, and we demonstrate the formation of heteronuclear molecules by a magnetic field ramp across the resonance.

The groundbreaking achievements in experiments with ultracold Fermi gases [Ing08, Gio08] have opened up unprecedented possibilities to study new regimes of strongly interacting quantum matter. Ultracold gases represent well-controllable model systems for the exploration of many-body regimes in a way not possible in conventional condensed-matter systems [Blo08]. A new frontier in the field is currently being explored in experiments on ultracold Fermi-Fermi mixtures of ^{6}Li and ^{40}K atoms [Tag08, Wil08, Voi09, Spi09, Tie10]. Because of the mass imbalance and the possibility to apply species-specific optical potentials, such

[†] The author of the present thesis carried out all experiments described in this article. He also analyzed the data with help by A.T. on the temperature fits.

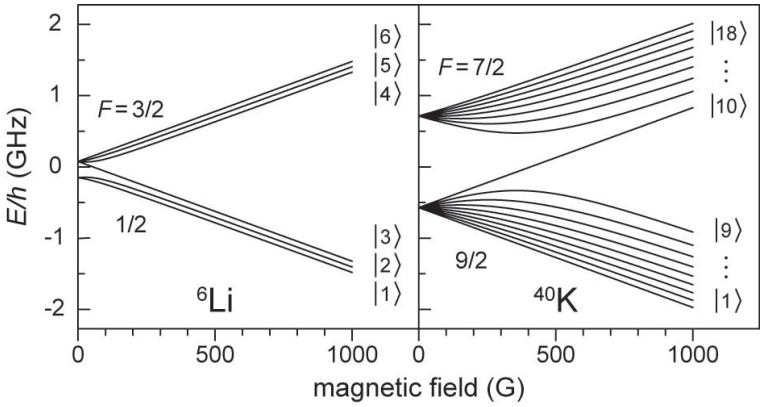

Figure 4.1. Electronic ground state energies of ^{6}Li and ^{40}K versus magnetic field.

systems promise manifold intriguing applications both in many-body physics [Paa06, Isk06, Isk07a, Pet07, Isk08c, Bar08, Bau09, Nis09a, Wan09, Mor09] and few-body physics [Pet05, Nis09b, Lev09].

To prepare degenerate Fermi gases, all-optical approaches have proven to be simple and robust and they facilitate highly efficient evaporative cooling. Therefore they are routinely applied in many present experiments; see Ref. [Ing08] for a review of earlier work and Refs. [Fuc07, Ina08, Ott08, Huc09] for more recent examples. Spin mixtures of ^{6}Li atoms near a broad Feshbach resonance are particularly well suited for this cooling approach because of their exceptional collision properties, which offer extremely large cross sections for elastic collisions in combination with very weak inelastic decay. This favorable situation motivates the general idea of using the strongly interacting ^{6}Li gas as a cooling agent for sympathetic cooling of another species. Following this idea in Ref. [Spi09], we recently demonstrated the sympathetic cooling of ^{40}K atoms by an evaporatively cooled, optically trapped spin mixture of ^{6}Li, reaching the double-degenerate regime.

In this Article, we first present more details on our all-optical approach of preparing a double-degenerate Fermi-Fermi mixture of ^{6}Li and ^{40}K. We then show new results related to interactions and molecule formation near interspecies Feshbach resonances. In Sec. 4.1, we discuss our dual-species cooling and trapping setup and the special loading procedures used for the optical traps. In Sec. 4.2, we present an important preparation step where spin relaxation in the mixture brings the K atoms into their lowest internal state. In Sec. 4.3, we describe the combined evaporative and sympathetic cooling process. In Sec. 4.4, we show how the mixture can be prepared near interspecies Feshbach resonances. In Sec. 4.5, we finally demonstrate the creation of ultracold heteronuclear Fermi-Fermi molecules by Feshbach association methods.

4.1. Dual-species cooling and trapping setup and procedures

Here, we outline the basic concept of our dual-species setup (Sec. 4.1.1), and we present the special procedures applied to prepare the optically trapped mixture. In Sec. 4.1.2 we describe how we operate a dual-species magneto-optical trap (MOT). In Sec. 4.1.3 we present the optical dipole traps (ODT) used in the experiments. In Sec. 4.1.4 we discuss the special loading procedure for the ODT. The whole scheme is optimized for a large number of ^{6}Li atoms, as this species is used as the cooling agent for sympathetic cooling of ^{40}K into degeneracy [Spi09].

Figure 4.1 shows the atomic ground state energy structure of ^{6}Li and ^{40}K. We label the energy levels Li$|i\rangle$ and K$|j\rangle$, counting the states with rising energy. The hyperfine splitting of ^{6}Li is 228.2 MHz. For ^{40}K, the hyperfine structure is inverted and the splitting amounts to 1285.8 MHz [Ari77]. For the low-lying states with $i \leq 3$ and $j \leq 10$, the projection quantum numbers are given by $m_{\mathrm{Li}} = -i + 3/2$ and $m_{\mathrm{K}} = j - 11/2$.

4.1.1. Experimental setup

For the cooling and trapping of Li and K we apply standard laser cooling and trapping techniques [Met99] combining a Zeeman-slowed atomic beam and a dual-species MOT for initial collection of atoms in the vacuum chamber. A detailed description of the experimental setup and the laser systems can be found in Ref. [Wil09a]. A dual-species oven, which is connected to the main chamber via a differential pumping section, delivers a well-collimated atomic beam. We operate the oven with isotopically enriched samples containing 80% of ^{6}Li and 7% of ^{40}K. The Zeeman slower can cool both species individually with the respective settings of the magnetic field gradients. The central element of our vacuum chamber is a glass cell that allows for very good optical access. We achieve excellent vacuum conditions with a pressure on the order of 10^{-11} mbar.

For both species we use diode laser systems with one grating stabilized master oscillator in combination with tapered amplifiers. The Li (K) laser system provides 11 mW (12 mW) per MOT beam and 80 mW (100 mW) for the Zeeman slower beam. Figure 4.2 shows a schematic drawing of the atomic energy levels and optical transitions used for cooling and trapping of Li and K. The Li MOT laser beams contain two frequency parts tuned to the cooling ($F = 3/2 \rightarrow F' = 5/2$) and repumping ($F = 1/2 \rightarrow F' = 3/2$) transitions and having equal power. For K the cooling ($F = 9/2 \rightarrow F' = 11/2$) to repumper ($F = 7/2 \rightarrow F' = 9/2$) ratio is three to two.

4.1.2. MOT loading

The initial collection and cooling of ^{6}Li and ^{40}K is achieved by conventional laser-cooling and trapping techniques. As loading of both species requires different settings of the Zeeman slower magnetic field, we use a sequential MOT-loading

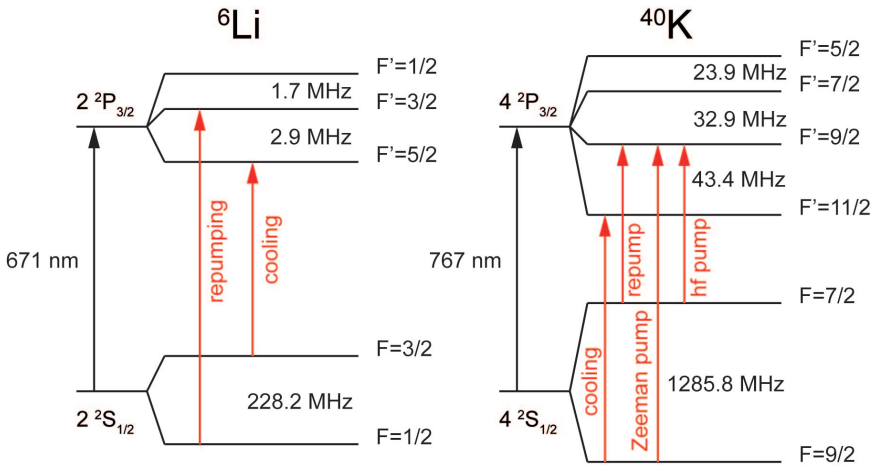

Figure 4.2. Scheme of the atomic energy levels and transitions used to cool and trap Li and K. Also shown are the transitions used for hyperfine (hf) and Zeeman pumping of K.

scheme. The basic idea is to first load Li and then add K in the presence of the Li MOT.

The Li MOT is operated with a field gradient of 26 G/cm along the symmetry axis of the field coils and a laser detuning of −27 MHz, for both, cooling and repumping transition. After a loading time of about 15 s, a few 10^9 Li atoms are accumulated in the MOT. At this point we increase the magnetic field gradient to 38 G/cm, where the K MOT works optimally. In 5 s, about 10^7 K atoms are added to the trap. The K MOT is operated with a laser detuning of −34 MHz.

During the K loading phase we operate the Li MOT with a relatively large detuning of −31 MHz in order to compensate for the effect of the higher magnetic field gradient on volume and density. This avoids increased losses by inelastic interspecies collisions, enabling the efficient sequential loading of both species.

In order to reduce shot-to-shot fluctuations of the number of atoms in the trap, we control the Li and K MOT loading by monitoring their fluorescence independently. When the fluorescence of the Li MOT reaches its threshold value, Li loading is stopped and loading of the K MOT is initiated. Once the K MOT fluorescence reaches its threshold, the K loading is turned off. At this point the ODT is ramped on in 100 ms, and the magnetic fields of the Zeeman slower are ramped to zero in 10 ms.

4.1.3. Optical dipole trapping schemes

For further storage and cooling of the atomic cloud, we use a trapping scheme that employs the optical dipole force of an intense infrared laser beam [Gri00] and the magnetic force in the curvature of the magnetic field [Joc03]. The latter becomes important when the optical trap is operated with low laser power. A schematic drawing of this hybrid trapping scheme is shown in Fig. 4.3.

The principal ODT is formed by a single beam (beam 1) delivered by a 200-W

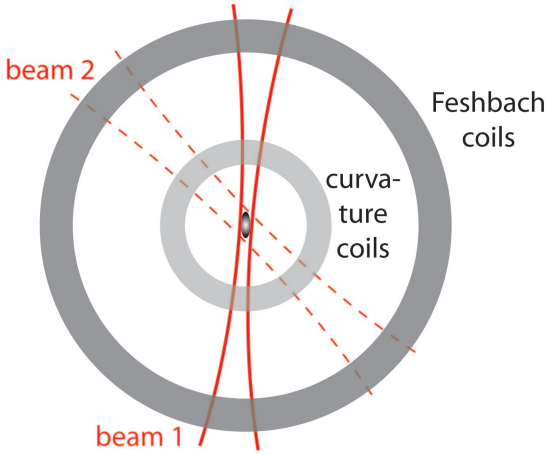

Figure 4.3. Schematic view of the optical trapping beam (beam 1) and the coils for the bias field and magnetic field curvature (shaded areas). Optionally, a second beam (beam 2) can be used for additional axial confinement.

fiber laser that emits light at a central wavelength of 1070 nm (IPG YLR-200SM-LP). The beam is focused down to a waist of 38 μm at the center of the MOT. During loading, the trap is operated with an optical power of 96 W, which results in a depth of 2.6 mK for Li. For K the trap depth is larger by a factor of 2.1 and thus amounts to about 5.5 mK.

Two sets of magnetic field coils are used in our setup to control the bias and curvature field independently; the coils setup is described in more detail in Appendix 4.A. For small bias fields the magnetic confinement is very small in the axial direction; here additional axial confinement can be obtained from another infrared beam (beam 2) delivered by a 5-W fiber laser with a central wavelength of 1065 nm (IPG YLP-5-LP). The single beam is focused to a waist of 97 μm and intersects beam 1 at an angle of 53°.

4.1.4. Dipole trap loading

Loading cold atoms of a single species from a MOT into a dipole trap is a standard procedure in many experiments. Sub-Doppler cooling and MOT compression are common methods to enhance transfer into the optical trap. The optimized loading of two species, however, needs special procedures. Here we describe the sequential loading scheme that gives us excellent starting conditions for the evaporation of Li and K in a common optical trap. A schematic illustration of the loading and transfer sequence is shown in Fig. 4.4. We found that an optimum is achieved by first transferring K into the optical trap while keeping Li stored in the large-volume, low-density MOT and then performing the Li transfer.

After switching on the ODT, in a first step the K MOT is compressed by ramping up the magnetic field gradient within 50 ms to 96 G/cm and bringing the frequencies of the K lasers closer to resonance to a detuning of a few MHz with an intensity lowered to 70%. At the same time the detuning of the Li MOT is increased to −47 MHz to

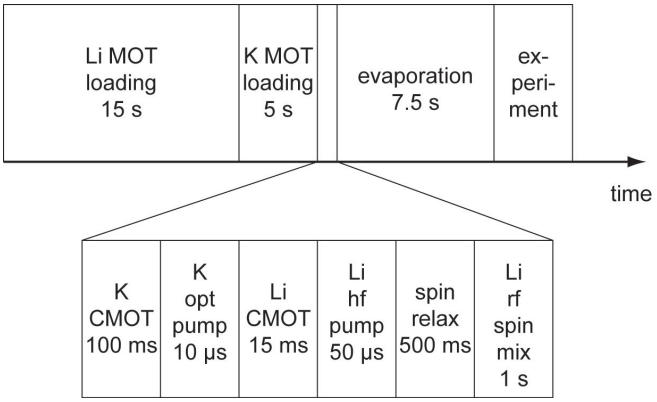

Figure 4.4. Illustration of the loading, transfer and measurement timing sequence. CMOT is an abbreviation for compressed MOT.

avoid compression of the Li MOT. At this point the K MOT light is extinguished and the K atoms are confined in the dipole trap while Li is stored practically undisturbed in a MOT at a reduced magnetic field gradient of 64 G/cm. With the K MOT beams off, untrapped atoms are allowed to escape for 50 ms.

Potassium has ten Zeeman sublevels in the lowest hyperfine ground state; see Fig. 4.1. In order to produce a spin-polarized sample of K in its lowest internal state, we apply an optical pumping scheme that not only transfers the atoms to the lower hyperfine state, but also pumps the atoms to the lowest m_F state.

For optical pumping the quadrupole field is switched off for 2 ms and only a small guiding field is kept on. Parallel to the field we shine in a σ^--polarized laser beam for 10 µs, which optically pumps the K atoms into state $|1\rangle$. The optical pumping beam contains two frequency components, one for Zeeman pumping tuned to the $(F = 9/2 \rightarrow F' = 9/2)$ transition and another one for hyperfine pumping tuned to the $(F = 7/2 \rightarrow F' = 9/2)$ transition as shown in Fig. 4.2. Each frequency component has about 50 times the saturation intensity. During the optical pumping stage, the cloud of Li atoms remains trapped in an optical molasses and can be recaptured without significant losses.

The high-power trapping laser induces a large light-shift on the optical cooling and pumping transitions. Potassium has two optical transitions between the excited $4^2P_{3/2}$ state and the $5^2S_{1/2}$ and $3^2D_{5/2}$ states with wavelengths of 1252 nm and 1177 nm, respectively. At high intensities of the ODT these two transitions shift the $4^2P_{3/2}$ level by several 100 MHz. Therefore optical pumping cannot be performed in the trap and we have to switch it off for a short time. After the 10 µs off-time of the ODT needed for the optical pumping, essentially all K atoms are recaptured into the ODT.

At this point we have a sample of a few 10^4 polarized ^{40}K atoms in the ODT, surrounded by a magneto-optically trapped cloud of ^{6}Li atoms. We finally apply a compressed MOT stage for Li in order to efficiently load this species into the dipole trap. For this, the quadrupole field is ramped back up to 64 G/cm and the MOT lasers are operated at a very small detuning of −3 MHz from resonance while the

power is lowered to 180 μW per beam for a duration of 15 ms. Hyperfine pumping of Li to the lower state is performed by switching the repumping laser off during the last 50 μs of the pulse. With this sequence we obtain a few 10^5 Li atoms in the lowest two spin states in the ODT at a temperature of about 300 μK.

4.2. Spin relaxation

A Li$|i\rangle$K$|j\rangle$ mixture can undergo rapid decay via spin relaxation if exoergic two-body collisions can take place that preserve the total projection quantum number $m_{\rm tot} = m_{\rm Li} + m_{\rm K} = -i + j - 4$. In such a process,

$$\mathrm{Li}|i\rangle + \mathrm{K}|j\rangle \rightarrow \mathrm{Li}|i-1\rangle + \mathrm{K}|j-1\rangle + E_r,$$

the energy E_r is released. Whenever one of the species is in the absolute ground state, and the other one is in a low-lying state ($i = 1$ and $j \leq 10$ or $j = 1$ and $i \leq 3$), spin relaxation is strongly suppressed [Sim03].

Since optical Zeeman pumping does not lead to a perfect transfer of all K atoms into the lowest spin state, we exploit spin relaxation to fully spin polarize K into state $|1\rangle$. We investigated the conditions under which spin relaxation can be used for this purpose. In these measurements we apply only hyperfine pumping, but no Zeeman pumping. We start with an almost equal mixture of Li in its lowest two hyperfine states, $|1\rangle$ and $|2\rangle$, trapped together with a population of K in all Zeeman substates $j \leqslant 10$.

We investigate the magnetic field dependence of the spin relaxation by holding the sample for 500 ms at a variable magnetic field. The trap is operated under the same conditions as during trap loading, i.e. with a trap depth of 2.6 mK for Li and 5.5 mK for K. The atom numbers are measured using spin-selective absorption images, which are always taken at a bias field of 1190 G [1]. Figure 4.5 shows the resulting atom numbers of Li in states $|1\rangle$ (open squares) and $|2\rangle$ (filled squares) as well as K in state $|1\rangle$ (filled circles). Two distinct peaks in the K$|1\rangle$ atom number are visible at 40 G and 207 G and coincide with dips in the Li$|2\rangle$ atom number. These features are fitted with Lorentzians to determine their positions and widths.

The release energy E_r at 40 G (207 G) corresponds to 2.1 mK (5.8 mK). For an inelastic collision between two atoms with different masses, the resulting kinetic energy contributions are inversely proportional to the mass. For the ^{6}Li-^{40}K combination, 87% of the released energy is transferred to the lighter Li atoms (mass $M_{\rm Li}$) and only 13% to the heavier K (mass $M_{\rm K}$). A necessary condition for the trap depth $U_{\rm K}$ under which a K atom stays confined is

$$U_{\rm K} > \frac{M_{\rm Li}}{M_{\rm K} + M_{\rm Li}} E_r, \tag{4.1}$$

[1] We use high-field imaging at 1190 G where the scattering length between Li$|1\rangle$ and $|2\rangle$ is small and negative. The Li cloud can thus be approximated as a weakly-interacting Fermi gas which in the degenerate regime allows for easier interpretation of the profiles obtained by absorption images after time-of-flight.

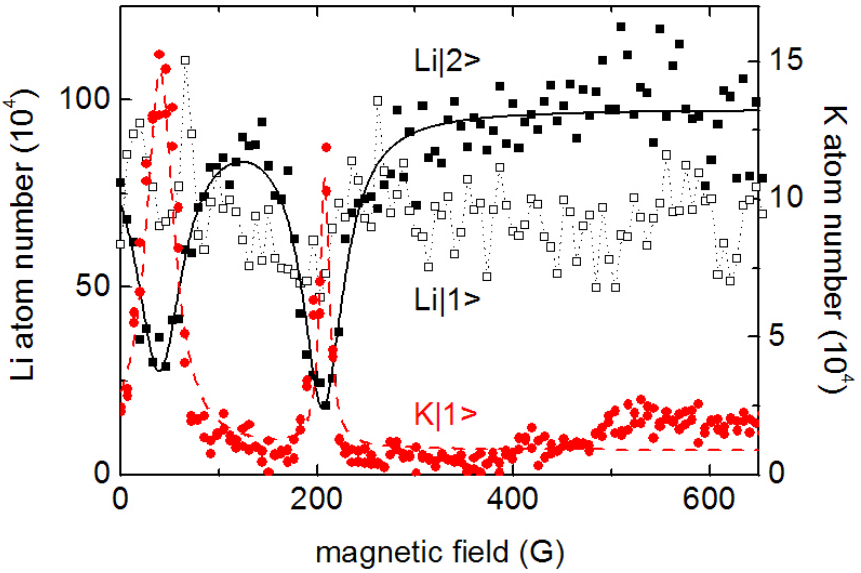

Figure 4.5. Magnetic field dependence of spin relaxation. The numbers of atoms in different spin states are measured by state-selective absorption imaging after a storage time of 500 ms in the dipole trap. The filled (open) squares give the Li$|2\rangle$ ($|1\rangle$) atom number, the filled circles are K$|1\rangle$. The two pronounced features that are visible at 40 G and 207 G are fitted by Lorentzians to determine their positions and widths.

and analogously for U_{Li}. The mass factor along with the about two times larger trap depth for K explains why we observe loss of Li atoms during the spin relaxation while K stays trapped. Furthermore, a K atom in a Zeeman level higher than $|2\rangle$ will need multiple collisions with Li$|2\rangle$ in order to fully polarize. That explains why much more Li$|2\rangle$ is lost than K$|1\rangle$ is gained during this process.

We interpret our data by comparing the position of the two spin relaxation features with the location of known interspecies Feshbach resonances, since we expect enhanced inelastic loss close to a Feshbach resonance [Chi10]. As Fig. 4.6 shows, there is a series of s-wave Feshbach resonances between Li$|2\rangle$ and K$|2 \leq j \leq 10\rangle$ near the 207 G feature. The distribution of Feshbach resonances coincides with the width of the observed spin relaxation feature. Note that the experiment is performed at relatively high temperature causing considerable broadening of the Feshbach resonances. Therefore individual resonances cannot be resolved.

For the feature of enhanced spin relaxation at 40 G, there are no interspecies s- or p-wave Feshbach resonances and thus we cannot explain it by means of scattering resonances. However, at low magnetic fields B the release energy E_r increases $\propto B$, which leads to a corresponding increase in the density of continuum states in the decay channel. We speculate that the corresponding threshold behavior may explain the increase at lower fields. Then, already at a few ten Gauss the nuclear spin of Li decouples from the electron spin, which may lead to a reduction of loss.

In a second set of experiments we investigate the time scale on which spin relaxation occurs at the two relevant magnetic fields 40 G and 207 G. For both fields we find that the time scale for the process is 150 ms and a steady state is essentially

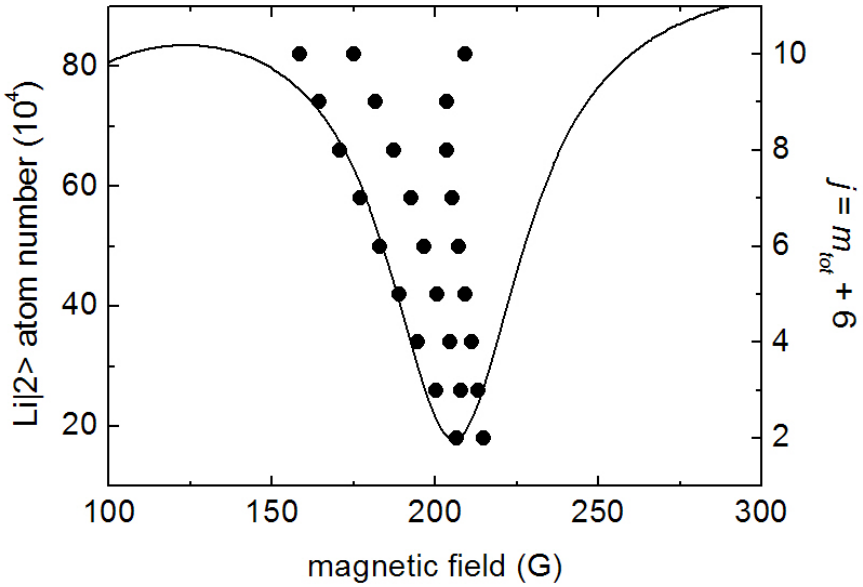

Figure 4.6. Interpretation of the 207 G spin relaxation feature in terms of Feshbach resonances. The dots show the calculated positions of Feshbach resonances between Li|2⟩ and K|2 ≤ j ≤ 10⟩ [Tie09]. Also plotted is the Lorentzian fit to the Li|2⟩ loss feature from Fig. 4.5 for comparison.

reached after 500 ms.

Spin relaxation is a very efficient process that allows us to fully polarize our K sample without loss of K atoms. Since initially much more Li atoms are present in the trap, the Li loss is a minor problem. The resulting imbalance of the two Li spin states can be removed by driving radio-frequency (rf) transitions between the two states.

4.3. Evaporation and sympathetic cooling

A spin-mixture of Li|1⟩ and Li|2⟩ near the broad 834-G Feshbach resonance facilitates highly efficient evaporative cooling, as it is well known in the field of strongly interacting Fermi gases [O'H02, Ing08]. The efficiency of the cooling process is due to the very favorable combination of a large elastic scattering cross section with very low losses. In Ref. [Spi09] we have already demonstrated the possibility of using the ^{6}Li spin-mixture as an efficient cooling agent to sympathetically cool another species. In this way we have demonstrated the attainment of a double-degenerate Fermi-Fermi mixture of ^{6}Li and ^{40}K. Here we present additional information on the experimental procedures, and the combined evaporative and sympathetic cooling process.

Let us first summarize our main findings of Ref. [Spi09] on the collisional stability of the three-component Fermi gas of Li in the lowest two spin states together with K in the lowest spin state. Interspecies collisional loss is negligible on the BCS side of the broad Li resonance ($B > 900$ G) and quite weak even exactly on resonance

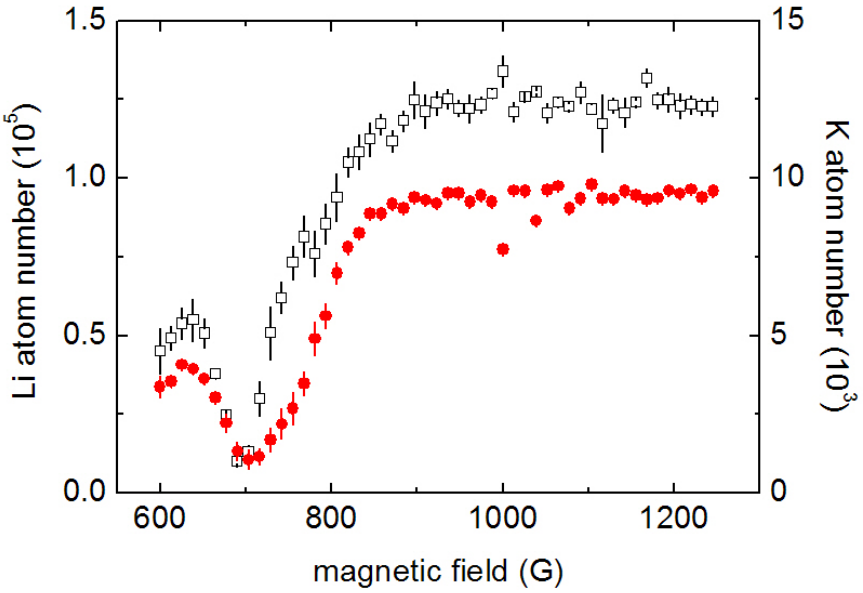

Figure 4.7. Li and K atom numbers after evaporation performed at variable magnetic field. Open squares show the number of Li atoms per state, filled circles show the K atom number.

(834 G). Substantial loss, however, occurs on the BEC side of the resonance in a range between about 650 and 800 G. The latter is a result of inelastic collisions between K atoms with weakly bound Li dimers. Consequently, the combined evaporation and sympathetic cooling process needs to be performed on the BCS side of the Li resonance. For our experiments we choose a field of 1190 G. Here the Li scattering length is $-2900\ a_0$ and the interspecies scattering length is about $+60\ a_0$.

Before starting the evaporation process, we carefully balance the population of the two spin states Li$|1\rangle$ and Li$|2\rangle$. This is particularly important in cases when the spin relaxation stage has caused considerable losses in $|2\rangle$. The spin balance is accomplished by driving the rf transition $|1\rangle \leftrightarrow |2\rangle$ using a series of 20 ramps over 10 kHz with a duration of 50 ms each [Str03]. This procedure is performed at 1190 G, where the Li spin mixture is outside of the strongly interacting regime and interaction-induced rf line shifts are relatively small. Note that the evaporation process is much more sensitive to a spin imbalance on the BCS side of the resonance than on the BEC side of the resonance. The reason is that in the latter case the molecule formation can lead to a self-balancing of the spin population during evaporation [Gri06].

Evaporation of the mixture is performed in the principal ODT, beam 1. The evaporation ramp consists of two stages, technically implemented in different ways. In the first stage, we use a digital input of the laser control unit to reduce the ODT power to about 15 W. This ramp is linear and takes 1.5 s. In a second stage, an acousto-optical modulator (AOM) is used to decrease the power in a nearly exponential ramp. The evaporation ramp is typically stopped after 6 s when the laser power is 60 mW. At this point the trap frequencies in the radial directions are 394 Hz for Li and 219 Hz for K. In the axial direction the trap frequency is dominated

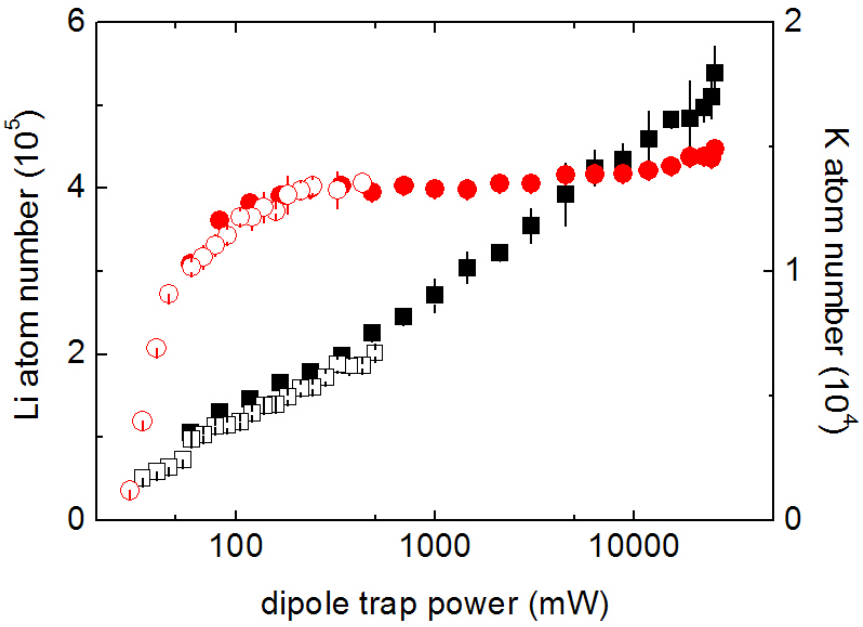

Figure 4.8. Evolution of the atom numbers during the second stage of evaporation. The Li atom number per state is plotted using squares while circles represent the K atom number. Filled (open) symbols represent data from measurements using fluorescence (absorption) imaging.

by the magnetic confinement and is 27 Hz for Li and 11 Hz for K.

The experimental data in Fig. 4.7 show the number of atoms remaining after the complete evaporation ramp for a magnetic field varied across the full tuning range offered by the Li Feshbach resonance. The data correspond to the observations of Ref. [Spi09], showing pronounced loss on the BEC side of the Li Feshbach resonance and large stability on its BCS side. In the high-field region between 950 G and 1250 G, where the Li scattering length varies between $-5300\ a_0$ and $-2800\ a_0$, the magnetic field has no significant influence.

In order to analyze the cooling process, we stop the evaporation ramp at a variable endpoint and measure the number of Li and K atoms. The measurements are performed by recapture into the MOT and subsequent detection of the fluorescence intensity or, at lower power, by absorption imaging after release from the ODT into free space. Figure 4.8 shows that the Li atom number steadily decreases while the K cooling proceeds essentially without losses. Note that the trap depth for K is a factor of 2.1 larger than for Li. This changes at about 100 mW, as the gravitational sag of K reduces the trap depth and we begin to see significant loss of K when further lowering the power of the ODT.

Figure 4.9 shows the temperature evolution of Li and K in the last part of the evaporation ramp. We extract the Li temperature by fitting a Thomas-Fermi profile to absorption images of the atomic cloud after time of flight. The K temperature is determined using a simple Gaussian fit, as the sample here remains in the non-degenerate regime. Throughout the whole evaporation the temperature of K lags

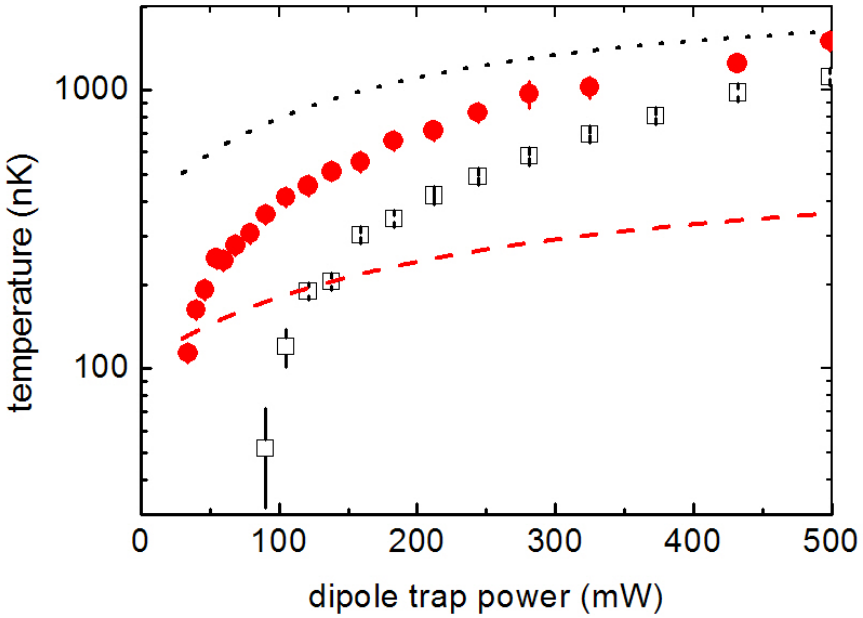

Figure 4.9. Temperature evolution during the last part of the evaporation. Open squares (filled circles) indicate the Li (K) temperature. Also plotted are curves that represent the evolution of the Fermi temperature for Li (dotted line) and K (dashed line).

behind the temperature of Li.

At the end of an extended evaporation ramp, at a trap power of 40 mW, the radial trap frequencies for Li (K) amounts to 320 Hz (160 Hz). In the axial direction the trap frequency is dominated by the magnetic confinement and is 27 Hz for Li and 11 Hz for K. The Fermi temperatures are calculated to be $T_F^{\mathrm{Li}} = 390\,\mathrm{nK}$ for Li and $T_F^{\mathrm{K}} = 135\,\mathrm{nK}$ for K. Following the scheme we have presented in Ref. [Spi09], we continue cooling of the mixture by holding it in this shallow trap for 5 s. This way we achieve a final K temperature of 50 nK corresponding to a degeneracy of $T^{\mathrm{K}}/T_F^{\mathrm{K}} \approx 0.6$ while Li is deeply degenerate with $T^{\mathrm{Li}}/T_F^{\mathrm{Li}} < 0.2$.

Since Li is the coolant of our evaporation scheme, we adjust the amount of K with which evaporation starts such that at the end of evaporation we have about ten times more atoms of Li in each spin state than atoms in K$|1\rangle$. In this situation K can be used as a probe for the Li mixture. One example of this idea has already been presented in Ref. [Spi09]. The measurement of the K temperature was used in order to get a firm upper bound for the temperature of the Li bath even in the strongly interacting regime. This method was recently adopted to using ^{7}Li as a probe in Ref. [Nas09].

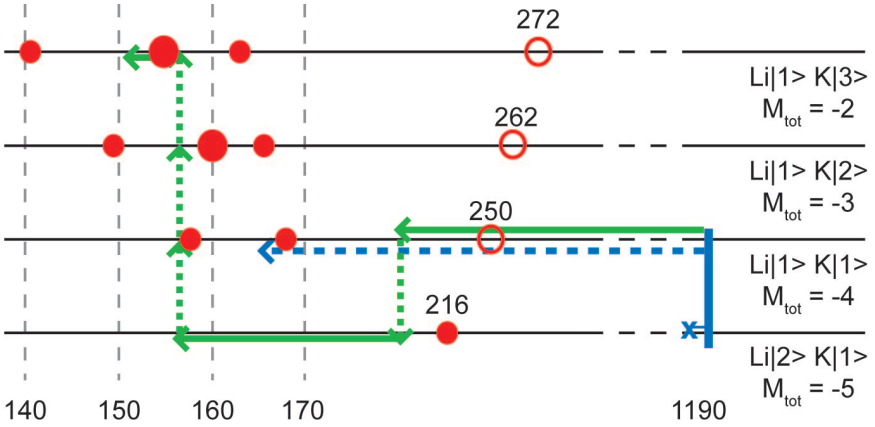

Figure 4.10. Preparation scheme of a two-component mixture near interspecies Feshbach resonances. The horizontal lines indicate four different Li-K spin channels being of particular relevance for our experiments. The numbers give the magnetic field values in Gauss. Filled (open) circles represent *s*-wave (*p*-wave) interspecies resonances. The Li|1⟩ and Li|2⟩ intraspecies *p*-wave resonances (not shown) are located at 160 G and 215 G respectively [Zha04, Sch05] and nearly coincide with interspecies resonances. For the *s*-wave resonances, the relative widths are indicated by the size of the symbols. State transfer, indicated by vertical dashed lines, is achieved by rf transitions. After the evaporation at 1190 G, the Li|2⟩ population is removed by a resonant laser pulse, as indicated by the **x**.

4.4. Preparation near interspecies Feshbach resonances

The ^{6}Li-^{40}K mixture offers several *s*-wave Feshbach resonances in the range between 150 G and 200 G [Wil08, Tie10]. All of them tend to be quite narrow, which is a common situation in cases of moderate values of the background scattering length [Chi10]. The broadest resonances were found for the channels Li|1⟩K|7...10⟩ with widths between 1 G and 2 G [Tie09]. The energetically lowest channel Li|1⟩K|1⟩, which is of particular interest because of the energetic suppression of any two-body decay, features two resonances with calculated widths around 100 mG. In this work, we focus on the resonance near 168 G. We show how a degenerate two-component Li-K mixture can be prepared near this resonance after sympathetic cooling at high magnetic field and present measurements on inelastic and elastic properties of the mixture.

When ramping down the magnetic field from its evaporation setting (1190 G) to the interspecies resonances, one has to cross the region of the broad 834-G Li|1⟩|2⟩ Feshbach resonance. If this spin channel is populated, the formation of ^{6}Li dimers inevitably leads to strong losses from the atomic sample. To avoid this problem, we remove one of the Li spin components by the light pressure of a resonant laser pulse [Du08] before starting the ramp. Note that already the momentum kick from one photon is sufficient to push a Li atom out of the shallow trap after evaporation. The pulse is applied for 10 µs with a few times the saturation intensity. We find that at

1190 G the interaction between the two spin components is weak enough to avoid any significant effect on the population in the remaining spin state. In this way, we reduce the three-component Fermi-Fermi gas to a two-component mixture.

To approach a specific interspecies resonance, it is also important to avoid the effect of other inter- and intraspecies resonances. We find that our ramps are fast enough (ramp speed up to 20 G/ms) to cross all the p-wave resonances without any problem. However, we find substantial losses on the interspecies s-wave resonances, even on the weaker ones. This already points to efficient molecule association [Chi10] as we will discuss in Sec. 4.5.

Figure 4.10 illustrates the procedures applied to reach specific interspecies Feshbach resonances. While it is straightforward to reach the 168-G resonance in the Li$|1\rangle$K$|1\rangle$ channel by a fast ramp after removal of the state Li$|2\rangle$, other resonances require more elaborate methods. As an example, we discuss the 155-G resonance in the Li$|1\rangle$K$|3\rangle$ channel, which is of interest as one of the broadest resonances (width between 0.5 and 1 G) in the low-lying spin channels. Here a possible way is to transfer the Li atoms from $|1\rangle$ to $|2\rangle$ after ramping down the field to ~200 G, thus converting the sample into a Li$|2\rangle$K$|1\rangle$ mixture. This can be done with very high efficiency using rf transfer methods. Then the ramp is continued down to a value close to 155 G and three subsequent rf transfers are applied to convert the population from Li$|2\rangle$K$|1\rangle$ to Li$|1\rangle$K$|3\rangle$. This procedure avoids all detrimental resonances. Analogous schemes can be applied to reach any other desired resonance.

In a set of experiments performed at the 168-G interspecies Feshbach resonance in the Li$|1\rangle$K$|1\rangle$ channel, we investigate aspects of inelastic and elastic collisions. Initially, we prepare about 2×10^5 Li atoms together with about 1.4×10^4 K atoms at a temperature of about 300 nK. The power of the trapping beam (beam 1) is 170 mW, corresponding to a radial (axial) trap frequency of 660 Hz (14 Hz) for Li. For K the trap frequencies are 375 Hz and 6 Hz respectively. The peak densities of the clouds are $n_0^{\mathrm{Li}}\approx 2\times10^{12}\,\mathrm{cm}^{-3}$ and $n_0^{\mathrm{K}}\approx 4\times10^{11}\,\mathrm{cm}^{-3}$ and the degeneracies are $T^{\mathrm{Li}}/T_F^{\mathrm{Li}}\approx 0.3$ and $T^{\mathrm{K}}/T_F^{\mathrm{K}}\approx 1.5$. Note that these conditions are deliberately prepared with an incomplete evaporation ramp, stopped at 170 mW instead of the usual final power of 60 mW (Sec. 4.3).

In the first series of measurements, we ramp the magnetic field to a variable value and study the loss of atoms after a hold time of 5 s. For detection, the remaining atoms are recaptured into the two-species MOT and their fluorescence is recorded. The K atom number, normalized to the background value away from resonance, is plotted in Fig. 4.11 (open squares). We observe a loss feature centered at 168.22 G. Ramping across the Feshbach resonance does not lead to loss, indicating that the phase-space density used in these experiments is insufficient for adiabatic molecule creation during the magnetic field ramp.

In the second series of measurements, we investigate whether an effect of enhanced elastic collisions can be observed in evaporative cooling near the interspecies resonance. Here we lower the power of beam 1 to 55 mW within 3 s, which results in a radial (axial) trap frequency of 375 Hz (14 Hz) for Li and 210 Hz (5 Hz) for K. As before, the number of remaining atoms is determined by recapture into a MOT and fluorescence detection. The corresponding data, plotted in Fig. 4.11

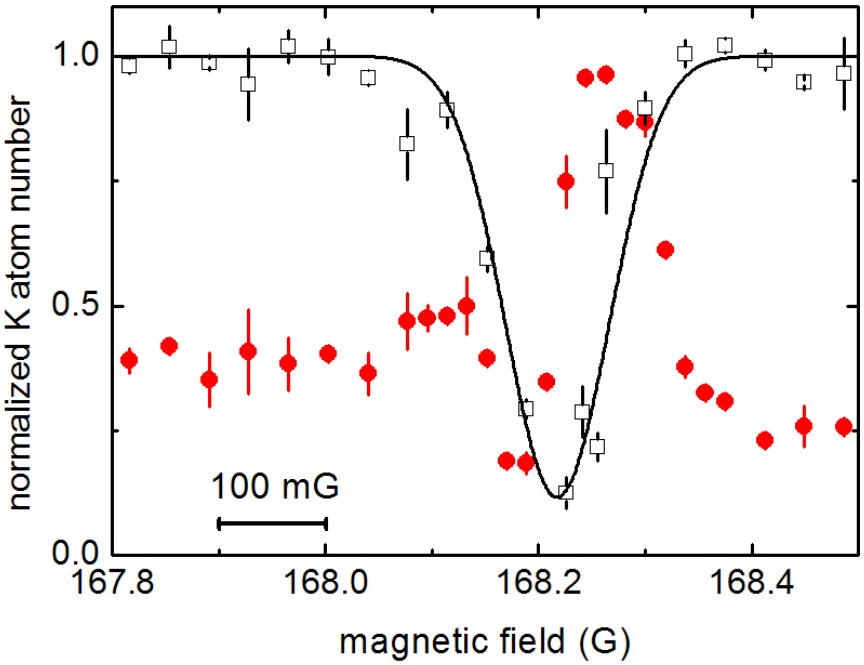

Figure 4.11. Loss measurement and evaporative cooling near an interspecies Feshbach resonance. Plotted is the K atom number normalized to the background value of the loss measurement away from resonance. The open squares show a set of loss measurements holding the sample at variable magnetic field for 5 s. The solid line is a Gaussian fit to the data. The filled circles show a corresponding set of measurements where evaporation was performed by lowering the optical power to one third of its initial value within 3 s.

(filled circles), show a pronounced asymmetry and thus a different behavior on the two sides of the Feshbach resonance. On its high-field side, corresponding to large negative scattering length, we observe a maximum in the recaptured atom number at 168.26 G. This signifies evaporative cooling with an enhanced elastic scattering cross section as compared to the background value. At lower fields, however, loss enhanced by the resonance dominates and leads to a minimum in atom number at 168.18 G. The loss properties on the two sides of the Feshbach resonance are thus found to be strikingly different with more favorable conditions on the side of negative scattering length, where no weakly bound molecular state exists.

To determine the resonance position more precisely, we prepare a sample with higher phase-space density than used for the previous sets of experiments. Now both beams of the ODT are used. Beam 2 is held at a constant power of 250 mW, corresponding to a trap depth of 1 μK for Li and 2.1 μK for K. Its purpose is to add confinement along the weak direction of beam 1 at the very end of evaporation. Evaporation at 1190 G and the ramp to low magnetic field proceed as described above. For further cooling, we create a balanced mixture of Li$|1\rangle$ and $|2\rangle$ at 170.5 G, using a sequence of rf sweeps. Afterwards, beam 1 is ramped from a Li trap depth of 1.9 μK to 1.5 μK during one second and the sample is left to thermalize for another second. Then Li$|2\rangle$ is removed by a short pulse of resonant light. At this point the

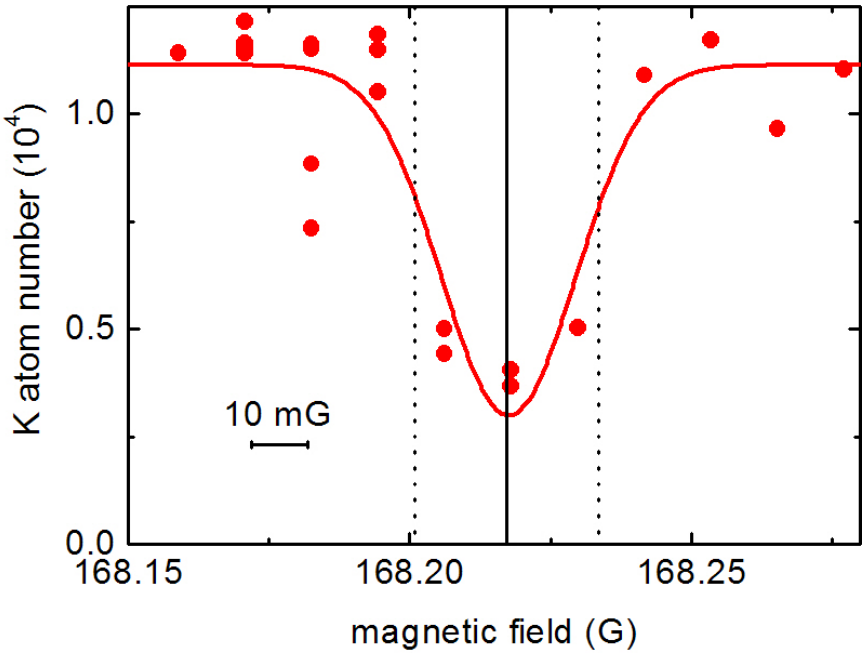

Figure 4.12. Scan of the Li-K Feshbach resonance at 168 G with 10 ms hold time. The $1/e$-width of the loss feature (indicated by the dotted lines) is determined by fitting a Gaussian to the experimental data and amounts to 33 mG.

sample has a temperature of ~200 nK and contains about 1.5×10^4 K atoms and 8×10^4 Li atoms. With the trap oscillation frequencies of axially 90 Hz (50 Hz), and radially 390 Hz (210 Hz) for Li (K), we calculate Fermi temperatures of about 900 nK for Li and 290 nK for K, corresponding to $T^{\mathrm{Li}}/T_F^{\mathrm{Li}} \approx 0.2$ and $T^{\mathrm{K}}/T_F^{\mathrm{K}} \approx 0.7$. The K cloud has less than half the size of the Li cloud. For both components the density in the center of the trap is about $2 \times 10^{12}\,\mathrm{cm}^{-3}$.

Under these deep cooling conditions, we detect the fast atom loss as a function of the magnetic field. In order to approach the magnetic field value of interest without forming molecules, K is transferred into state $|2\rangle$ by an rf π-pulse prior to the magnetic field ramp. At the final field, K is transferred back to state $|1\rangle$ by another π-pulse. After a hold time of 10 ms, the remaining K atom number is measured. Figure 4.12 shows the corresponding data. We observe maximum loss of atoms centered at 168.217 G, with an estimated calibration uncertainty of 10 mG.

4.5. Creation of ultracold Fermi-Fermi molecules

Here, we describe our basic methodology for molecule creation and detection (Sec. 4.5.1), present experimental results (Sec. 4.5.2) and discuss our findings (Sec. 4.5.3).

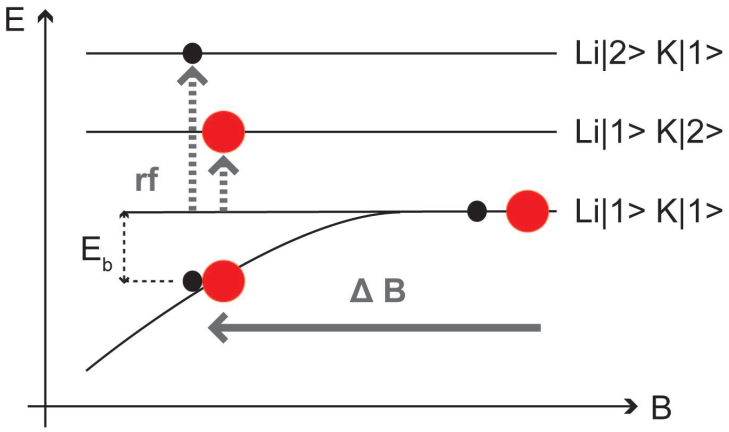

Figure 4.13. Molecules are associated by a magnetic field ramp, indicated by the arrow labeled ΔB, across a Feshbach resonance. Transitions to higher atomic spin states are driven by rf pulses. Atoms bound in a molecule are not affected because of the binding energy E_b.

4.5.1. Creation and detection schemes

The creation of the molecules starts with a Li$|1\rangle$K$|1\rangle$ mixture under the same conditions as prepared for Fig. 4.12. The molecules are associated by a magnetic field ramp from 170.5 G to 168.19 G within 10 ms, crossing the Li$|1\rangle$K$|1\rangle$ 168-G Feshbach resonance (ramp speed 0.23 G/ms). Instantly after the ramp, the sample is released from the ODT.

Selective imaging of molecules and remaining unpaired atoms is possible after transfer of the unpaired atoms to the states Li$|2\rangle$ and K$|2\rangle$. An rf π-pulse, tuned to the atomic $|1\rangle \rightarrow |2\rangle$ transition, is used for this purpose [2]; see Fig. 4.13. Atoms bound in LiK molecules are not transferred to state $|2\rangle$ if the molecular binding energy detunes the transition far enough from the free atom transition to be outside of the Fourier spectrum of the rf pulse. This condition requires a detuning of 23 kHz for K, which is reached 9 mG below resonance according to the relative magnetic moment of the molecular state [Tie09]. The rf pulses are applied one after the other during the 0.4 ms free expansion of the sample.

State-selective absorption images are taken simultaneously on cycling transitions starting from the Li$|1\rangle$ and K$|1\rangle$ states. This way, molecules are imaged directly. The resulting pictures are shown in the left-hand column of Fig. 4.14 [3]. A second pair

[2] The rf transition frequencies for Li and K are 39 MHz and 69 MHz, respectively. The π-pulses are approximately rectangular and have a total duration of 43 µs (333 µs) for K (Li). The duration of the Li pulse is much longer than that of the K pulse, because less rf power is available. The full width of the dominant central peak in the Fourier spectrum is 46 kHz for K and 6 kHz for Li. We can achieve transfer efficiencies higher than 99%.

[3] A slight off-resonant contribution of atoms in the K$|2\rangle$ state is visible on K$|1\rangle$ images. Since this contribution has a much larger spatial extent than the cloud of molecules, it is possible to correct for it when extracting data from the image. We also account for unpaired atoms not transferred by the rf pulse by independently measuring the π-pulse transfer efficiency.

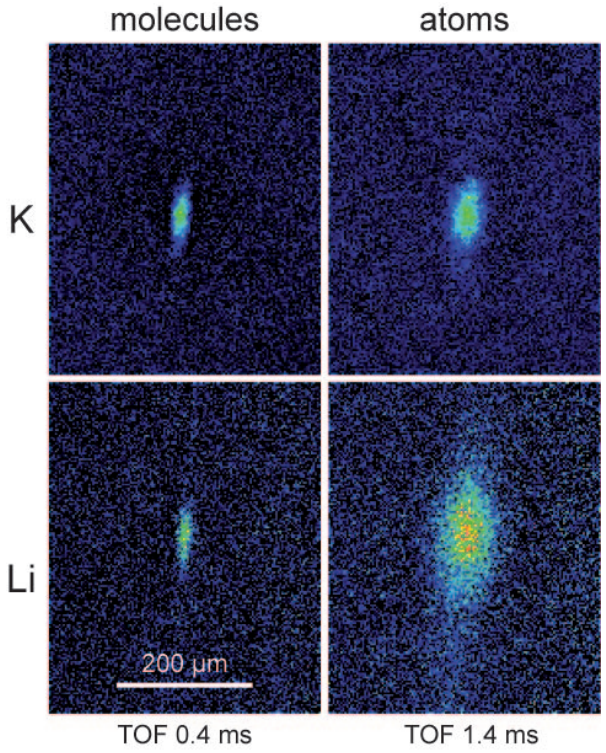

Figure 4.14. Absorption images of LiK Feshbach molecules and unpaired atoms taken at a magnetic field of 168.19 G. The upper row shows images of molecules and atoms taken with light resonant to the K transition whereas the lower row shows images taken with light resonant to the Li transition. The left column shows molecules imaged after 0.4 ms time of flight (TOF) expansion and the right column unpaired atoms imaged 1 ms later.

of images, this time of the unpaired atoms, which have been transferred to the $|2\rangle$ states, is taken 1 ms later and shown in the right-hand column of Fig. 4.14 [4].

Absorption imaging of the molecules gives lower boundaries $\mathcal{N}_{\rm mol}^{\rm K}$ and $\mathcal{N}_{\rm mol}^{\rm Li}$ for the real molecule numbers $N_{\rm mol}^{\rm K}$ and $N_{\rm mol}^{\rm Li}$ since the absorption cross section of atoms bound in LiK molecules is somewhat smaller than the one of unpaired atoms. Close to the Feshbach resonance the cross section is similar to the one of free atoms and decreases for increasing binding energy. The number of remaining unpaired atoms $N_{\rm free}^{\rm K}$ and $N_{\rm free}^{\rm Li}$ can be obtained from the second pair of absorption images.

From K images (top row of Fig. 4.14) we obtain $\mathcal{N}_{\rm mol}^{\rm K} = 3\times10^3$ and $N_{\rm free}^{\rm K} = 9\times10^3$ and from Li images (bottom row of Fig. 4.14) $\mathcal{N}_{\rm mol}^{\rm Li} = 4\times10^3$ and $N_{\rm free}^{\rm Li} = 8\times10^5$. The small cloud of K is immersed in a much larger degenerate Li bath. The molecule conversion efficiency is therefore best characterized by the K conversion efficiency. A lower bound for the molecule fraction can be determined from K absorption

[4] Li$|2\rangle$ atoms are directly imaged using a probe beam of appropriate frequency. Since we do not have a probe beam with the correct frequency to image K$|2\rangle$ atoms, we first transfer those atoms back to state $|1\rangle$ using another π-pulse and then take the image using the same K$|1\rangle$ probe beam as before. Atoms imaged on the first set of pictures have been accelerated and heated by the probe beam flash and have dispersed enough at the time the second image is taken to not influence it.

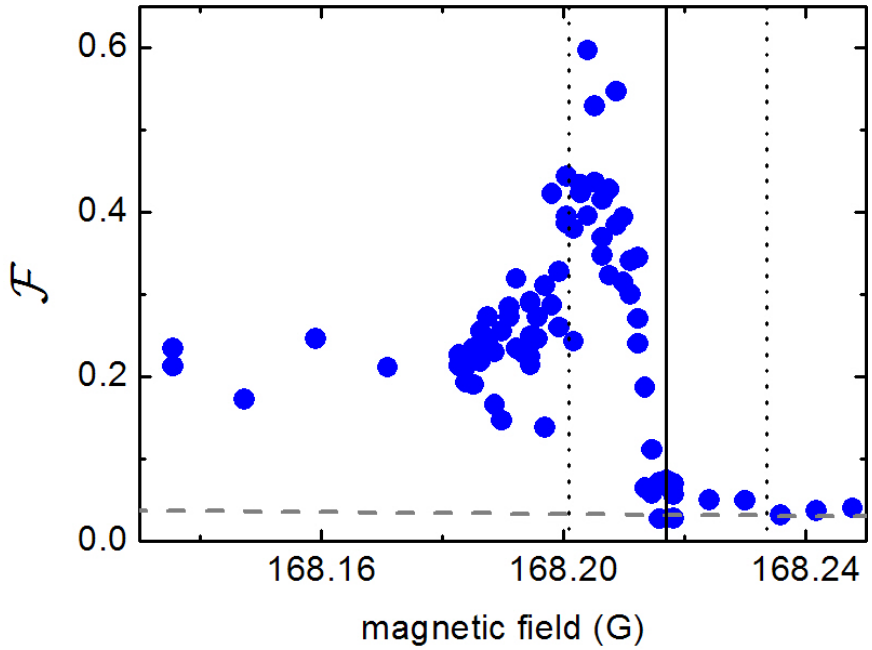

Figure 4.15. Lower bound of molecule fraction $\mathcal{F}$ in dependence of the final magnetic field value of the molecule association magnetic field ramp. Molecules are detected for fields below 168.218 G. This field corresponds to the center of the loss feature shown in Fig. 4.12, which is marked by the vertical solid line here. The dashed vertical lines mark the $1/e$-width of the loss feature and the horizontal dashed line marks a systematic offset.

images as $\mathcal{F} = \mathcal{N}^{\mathrm{K}}_{\mathrm{mol}}/(\mathcal{N}^{\mathrm{K}}_{\mathrm{mol}} + N^{\mathrm{K}}_{\mathrm{free}})$. From the images shown in Fig. 4.14 we obtain $\mathcal{F} = 0.25$.

4.5.2. Experimental results

We now examine the molecule creation process and properties of the molecules in more detail. First, we determine the magnetic field value of the onset of molecule creation. For this, we perform experiments as the one just described, but we vary the endpoint of the magnetic field ramp, keeping the ramp duration fixed. The frequency of the rf pulse for the separation of free K atoms and LiK molecules and the probe beam frequencies are adapted accordingly. The Li rf pulse was not used in these experiments.

Figure 4.15 shows the lower bound for the molecule fraction $\mathcal{F}$. Imperfect rf pulses lead to a 3% systematic offset in the data, indicated by the horizontal dashed line [5]. It is found that the detected molecule fraction depends strongly on the endpoint of the magnetic field ramp. No molecules are detected down to a final

[5] The offset in dependence of the magnetic field originates from imperfect frequency adjustment of the K π-pulse and was determined by experiments during which molecule formation was inhibited by removing Li$|1\rangle$ from the sample with a short flash of resonant light before the molecule association magnetic field ramp. The offset is 1% at 168.9 G and rises to 10% 1.5 G away from that position.

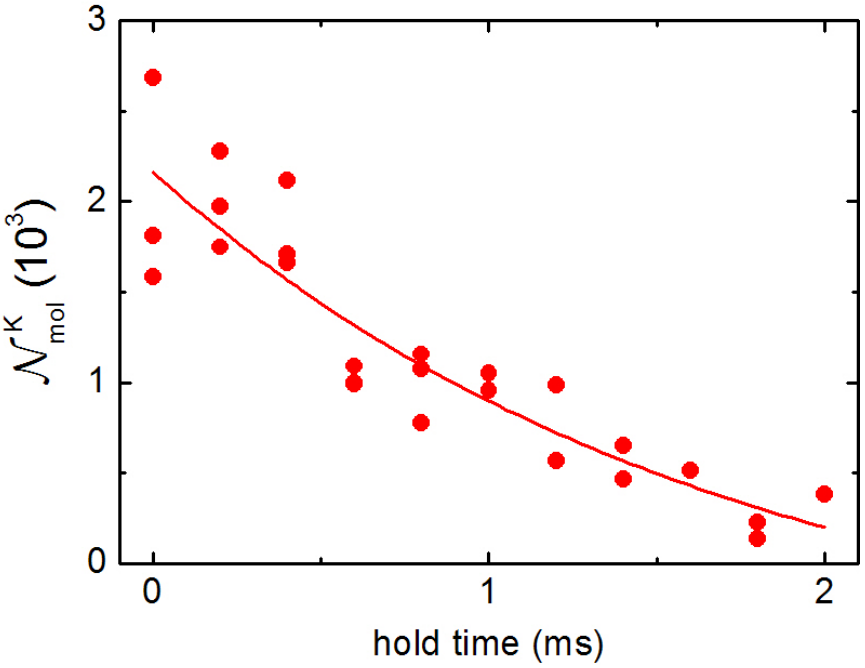

Figure 4.16. Decay of LiK molecules at 168.204 G. Plotted is the number of molecules $\mathcal{N}^{\mathrm{K}}_{\mathrm{mol}}$ in dependence on the hold time after the fast magnetic field ramp. The solid line is an exponential fit to the data, yielding a lifetime of 1.7 ms.

field of 168.217 G. Only 13 mG lower the maximum molecule fraction is observed. This magnetic field range corresponds well to the required detuning from resonance for our atom-molecule separation method to work, as discussed above. For lower fields the molecular signal drops again, first steeply down to about 168.19 G and then much slower. At about 167.5 G (outside the range of the plotted data) it becomes indiscernible from the background noise. The dependence of the detected molecule fraction on the field may have several reasons. It might be caused by the change in absorption cross section of the molecules with the magnetic field. The slow decrease away from resonance comes from loss of molecules as more time is spent between molecule association and detection.

Within the measurement precision of a few mG the onset of molecule detection coincides with the center of the loss feature from Fig. 4.12, marked by the solid vertical line in Fig. 4.15. This observation is in accordance with the standard picture of molecule formation close to a Feshbach resonance [Köh06].

The maximum K molecule conversion efficiency extracted from this data is reached at 168.204 G and amounts to about 40%. A different method to determine the K molecule conversion efficiency is to examine the number of free K atoms at a magnetic field just above the onset of molecule production and just below 168.19 G. Assuming all missing atoms have formed molecules, the molecule conversion efficiency is also determined to be 40%. The assumption that no molecules are lost is well justified since the time spent in the Feshbach resonance region during the magnetic field ramp to 168.19 G (120 µs) is short compared to the lifetime of the

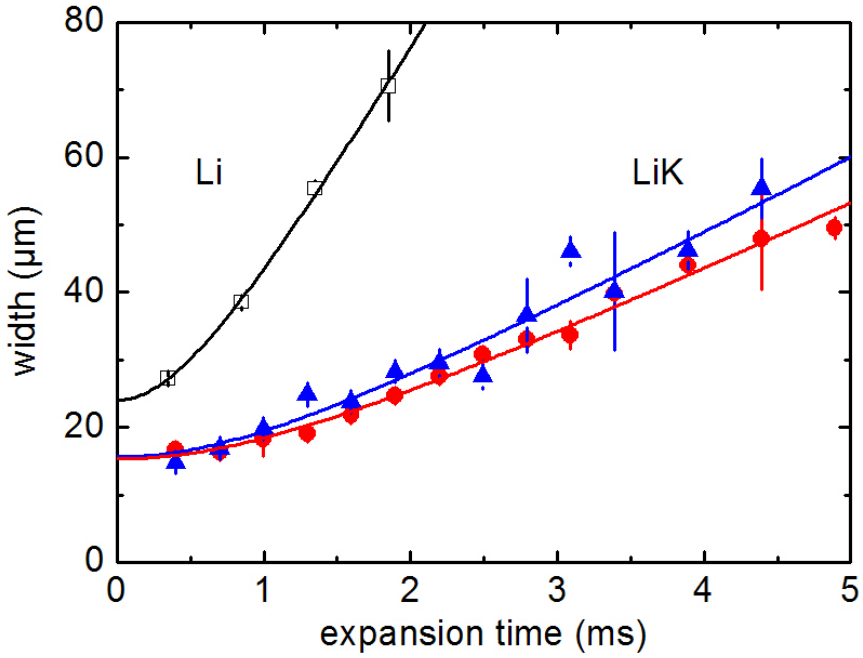

Figure 4.17. Comparison of the free expansion of LiK Feshbach molecules (circles: detection of the bound K atoms, triangles: detection of the bound Li atoms) and unpaired Li atoms (open squares) at 168.196 G. Shown is the radial $1/\sqrt{e}$-width of Gaussian fits to integrated density profiles.

molecules.

The lifetime of the LiK molecules is determined by holding the sample after molecule creation for a varying time in the ODT at a constant magnetic field of 168.204 G and measuring the molecule number afterwards. A fit to the decay of the molecule number gives a lifetime of 1.7 ms; see Fig. 4.16. This lifetime does not change if the remaining free Li atoms are removed just after molecule creation by a resonant flash of light, indicating that the dominant loss mechanism does not involve free Li atoms. We did not investigate the effect of unpaired K atoms on the molecule lifetime.

A striking manifestation of molecule formation can be observed by comparing the expansion behavior of clouds of LiK molecules with the one of clouds of unpaired Li atoms in imaging with Li light. For this comparison, we record the expansion of the molecules and the remaining unpaired Li atoms after a molecule association magnetic field ramp to 168.196 G; see Fig. 4.17. We find the average expansion velocity of molecules to be slower by a factor of 3.3, as determined by fits to the expansion. We interpret this difference mainly as a result of the higher mass of the molecules compared to unpaired Li atoms. It corresponds well to the expected velocity ratio of $v_{\mathrm{Li}}/v_{\mathrm{LiK}} = \sqrt{M_{\mathrm{LiK}}/M_{\mathrm{Li}}} = \sqrt{46/6} = 2.8$ in the approximation of thermal clouds of equal temperature. This observation tells us that Li atoms that remain in state $|1\rangle$ after the π-pulse are bound to K atoms.

4.5.3. Discussion

In our experiment, molecule association is achieved in basically the same way as demonstrated in many other cold atom experiments before [Chi10, Köh06] and our results agree well with the standard picture of molecule formation close to a Feshbach resonance [Köh06]. We observe that molecule association is most efficient in samples of high phase-space density and obtain a maximum molecular conversion efficiency for K of 40%. This conversion efficiency is typical for experiments employing the Feshbach ramp technique. A Monte Carlo simulation based on the method presented in Ref. [Hod05] agrees with our results, giving a conversion efficiency of about 50% for K.

The lifetime of our molecules is quite short, only 1.7 ms. Because of this, it would be technically challenging to observe the standard signature of molecule association, which is the reduction of the absorption imaging signal when ramping to the molecular side of the Feshbach resonance and the recovery of the signal after ramping back. Our rf state separation detection technique, which allows to obtain images of molecules less than 0.1 ms after molecule association, overcomes this detection problem.

The Li$|1\rangle$K$|1\rangle$ molecule lifetime that we measure is much shorter than typical lifetimes of Li$|1\rangle$K$|3\rangle$ molecules that were measured by the Munich group [Voi09]. Presently, we do not know whether the different spin channels and therefore the different Feshbach resonances used for molecule association can explain the different lifetimes. There are also other possible, more technical reasons, which we presently cannot rule out. One possibility, which needs further investigation, is the loss of molecules because of the absorption of photons from the broad spectrum of the multi-mode fiber laser used for the ODT [6].

4.6. Conclusion & Outlook

We have presented an all-optical evaporative and sympathetic cooling scheme for the preparation of a double degenerate ^{6}Li-^{40}K Fermi-Fermi mixture. We have also shown the general methodology to prepare the sample close to specific interspecies Feshbach resonances. As a first application, we have demonstrated the formation of Fermi-Fermi heteronuclear molecules and we have examined the molecule association process and some properties of the molecules.

With the basic tools at hand, we are now in the position for the next steps towards our main goal to realize strongly interacting regimes in the Fermi-Fermi mixture. Since the available Feshbach resonances are quite narrow this requires precise knowledge of the exact resonance position and the magnetic-field dependent elastic and inelastic interaction properties. We are currently inspecting the relatively broad 155-G resonance in the Li$|1\rangle$-K$|3\rangle$ channel as a promising candidate, for which we experimentally find a width of about 800 mG [Nai10]. Strongly interacting

[6] A strong influence of broadband laser light on the lifetime of molecules was observed in experiments on cesium Feshbach molecules in Innsbruck. The lifetime substantially increased when the trapping light was provided by a single-mode infrared laser.

conditions generally require a scattering length exceeding the interparticle spacing. Under our typical experimental conditions this would be realized with a magnetic detuning below 10 mG, which is experimentally feasible.

We want to thank Paul Julienne for fruitful discussions and support on the theoretical understanding of the interspecies scattering properties, Tobias Tiecke for the calculated Feshbach resonance positions displayed in Fig. 4.6, Christoph Kohstall for useful comments on the manuscript, and Clarice Aiello for contributions to the experimental set-up. This work is supported by the Austrian Science Fund (FWF) and the European Science Foundation (ESF) within the EuroQUAM/FerMix project and by the FWF through the SFB FoQuS.

4.A. Magnetic field coils

Three pairs of magnetic field coils are present in the setup: a pair of high-current, large-diameter coils, which we call Feshbach coils, a smaller-diameter pair of high-current coils, which we call curvature coils, and a third, low-current, low inductance pair of coils, which we call fast coils. Normally, the currents in all coils circulate in the same direction. To achieve a quadrupole field configuration for MOT operation, the direction of current in one coil of the Feshbach coil pair and one coil of the curvature coil pair can be reversed using mechanical relays. In the normal configuration, the Feshbach coils are in Helmholtz configuration and give a very homogeneous bias field near the trap center of up to 3000 G. The curvature coils exhibit a magnetic field curvature, which gives rise to an additional contribution to the trapping potential [Joc03]. With the current used during evaporation, the curvature coils give a homogeneous bias field of 600 G and a magnetic field curvature of 27 G/cm^2 along the axial direction of the dipole trap beams (perpendicular to the symmetry axis of the coils). This curvature gives rise to a magnetic confinement corresponding to trap frequencies of 27 Hz for Li and 10 Hz for K. When working at bias fields between 150 G and 170 G, where the interspecies Feshbach resonances are, the curvature coils provide a magnetic confinement corresponding to 13 Hz for Li and 5 Hz for K.

When high magnetic field-stability is needed, we make use of a battery-powered current supply. Since the interspecies Feshbach resonances are very narrow, it is necessary to control the magnetic field with very high precision. Passive stabilization methods, not employing any shielding, lead to a stability of about 10 mG peak-to-peak over a 50 Hz cycle. By synchronizing the experimental sequence to line, we achieve a magnetic field stability of a few mG for times on the order of one ms, which is much larger than the typical duration of rf π-pulses we use for internal state transfer. Magnetic field values are calibrated using rf transitions.

For probing the interspecies resonances we make use of the fast coils, which have Helmholtz configuration. Using these coils we make precise magnetic field ramps of up to 3 G in about 0.1 ms. This response time of the magnetic field was characterized by measuring the change in frequency of an atomic RF transition with time after a step change of the current. The response time is not limited by the speed of change of the current through the coil, but by eddy currents.

APPENDIX A

LASER FREQUENCIES

In this Appendix some technical figures are documented as a reference for working in the laboratory. They are shown here because the author of the present thesis designed the laser setup that allows for imaging of Li and K at the magnetic fields of interest: the BEC-regime around 760 G, the BCS-regime around 1190 G and around the interspecies Feshbach resonances between 150 G and 170 G as well as at the Li Feshbach resonance at 834 G.

Figures A.1 and A.2 give a schematic view of the cooling and imaging frequencies that are used in the experiment and how they are generated by different acousto-optical modulators (AOMs) in the laser setup.

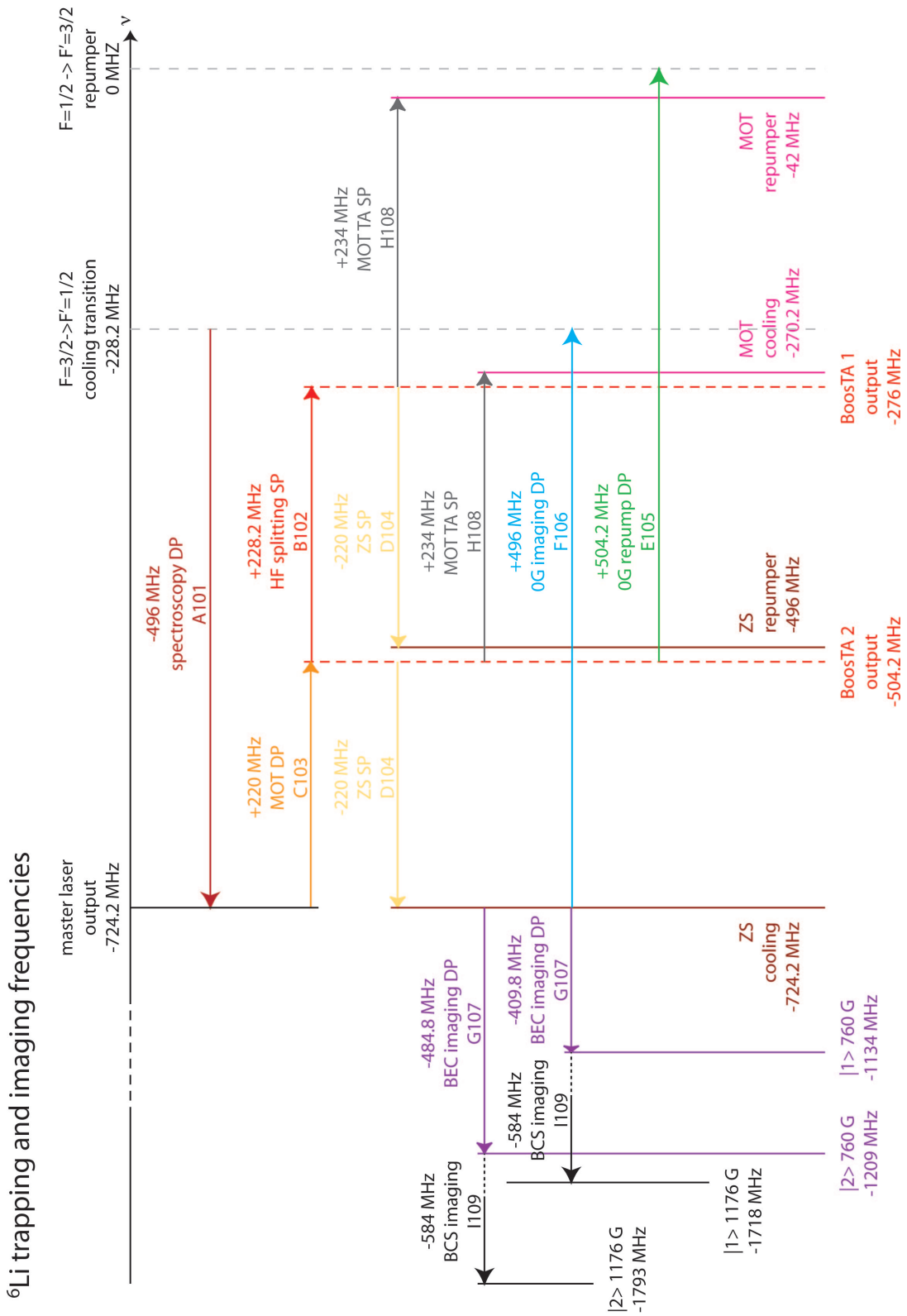

Figure A.1. Li cooling and imaging frequencies.

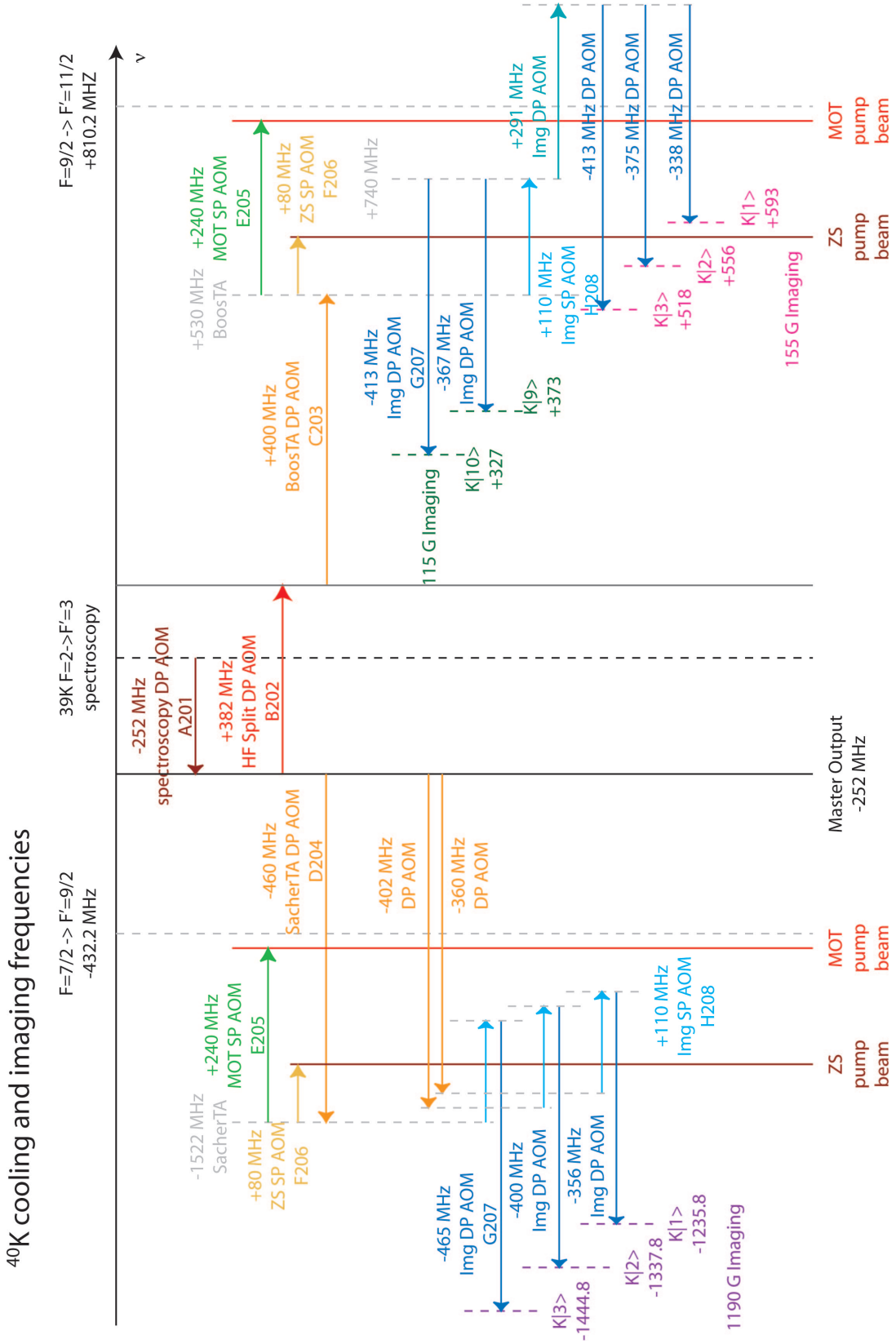

Figure A.2. K cooling and imaging frequencies.

BIBLIOGRAPHY

[Ari77] E. ARIMONDO, M. INGUSCIO and P. VIOLINO. Experimental determinations of the hyperfine structure in the alkali atoms. *Rev. Mod. Phys.* **49** (1977) 31.

[Aym05] M. AYMAR and O. DULIEU. Calculation of accurate permanent dipole moments of the lowest $^{1,3}\Sigma^{+}$ states of heteronuclear alkali dimers using extended basis sets. *J. Chem. Phys.* **122** (2005) 204302.

[Bar57a] J. BARDEEN, L. N. COOPER and J. R. SCHRIEFFER. Microscopic Theory of Superconductivity. *Phys. Rev* **106** (1957) 162.

[Bar57b] J. BARDEEN, L. N. COOPER and J. R. SCHRIEFFER. Theory of superconductivity. *Phys. Rev* **108** (1957) 1175.

[Bar04] M. BARTENSTEIN, A. ALTMEYER, S. RIEDL, S. JOCHIM, C. CHIN, J. HECKER DENSCHLAG and R. GRIMM. Crossover from a Molecular Bose-Einstein Condensate to a Degenerate Fermi Gas. *Phys. Rev. Lett.* **92** (2004) 120401.

[Bar05] M. BARTENSTEIN, A. ALTMEYER, S. RIEDL, R. GEURSEN, S. JOCHIM, C. CHIN, J. HECKER DENSCHLAG, R. GRIMM, A. SIMONI, E. TIESINGA, C. J. WILLIAMS and P. S. JULIENNE. Precise Determination of ^{6}Li Cold Collision Parameters by Radio-Frequency Spectroscopy on Weakly Bound Molecules. *Phys. Rev. Lett.* **94** (2005) 103201.

[Bar08] M. BARANOV, C. LOBO and G. V. SHLYAPNIKOV. Superfluid pairing between fermions with unequal masses. *Phys. Rev. A* **78** (2008) 033620.

[Bau09] I. BAUSMERTH, A. RECATI and S. STRINGARI. Chandrasekhar-Clogston limit and phase separation in Fermi mixtures at unitarity. *Phys. Rev. A* **79** (2009) 043622.

[Blo08] I. BLOCH, J. DALIBARD and W. ZWERGER. Many-body physics with ultracold gases. *Rev. Mod. Phys.* **80** (2008) 885.

[Bou03] T. BOURDEL, J. CUBIZOLLES, L. KHAYKOVICH, K. M. F. MAGALHAES, S. J. J. M. F. KOKKELMANS, G. V. SHLYAPNIKOV and C. SALOMON. Measurement of the Interaction Energy near a Feshbach Resonance in a ^{6}Li Fermi Gas. *Phys. Rev. Lett.* **91** (2003) 020402.

[Bou04] T. BOURDEL, L. KHAYKOVICH, J. CUBIZOLLES, J. ZHANG, F. CHEVY, M. TEICHMANN, L. TARRUELL, S. J. J. M. F. KOKKELMANS and C. SALOMON. Experimental Study of the BEC-BCS Crossover Region in Lithium 6. *Phys. Rev. Lett.* **93** (2004) 050401.

[Cas04] R. CASALBUONI and G. NARDULLI. Inhomogeneous superconductivity in condensed matter and QCD. *Rev. Mod. Phys.* **76** (2004) 263.

[Cha62] B. S. CHANDRASEKHAR. A note on the maximum critical field of high-field superconductors. *Appl. Phys. Lett.* **1** (1962) 7.

[Che05a] Q. CHEN, J. STAJIC and K. LEVIN. Thermodynamics of interacting fermions in atomic traps. *Phys. Rev. Lett.* **95** (2005) 260405.

[Che05b] F. CHEVY, E. G. M. VAN KEMPEN, T. BOURDEL, J. ZHANG, L. KHAYKOVICH, M. TEICHMANN, L. TARRUELL, S. J. J. M. F. KOKKELMANS and C. SALOMON. Resonant scattering properties close to a p-wave Feshbach resonance. *Phys. Rev. A* **71** (2005) 062710.

[Che06a] Q. CHEN, C. A. REGAL, D. S. JIN and K. LEVIN. Finite-temperature momentum distribution of a trapped Fermi gas. *Phys. Rev. A* **74** (2006) 011601.

[Che06b] F. CHEVY. Universal phase diagram of a strongly interacting Fermi gas with unbalanced spin populations. *Phys. Rev. A* **74** (2006) 063628.

[Chi04] C. CHIN, M. BARTENSTEIN, A. ALTMEYER, S. RIEDL, S. JOCHIM, J. HECKER DENSCHLAG and R. GRIMM. Observation of the Pairing Gap in a Strongly Interacting Fermi Gas. *Science* **305** (2004) 1128.

[Chi06] J. K. CHIN, D. E. MILLER, Y. LIU, C. A. STAN, W. SETIAWAN, C. SANNER, K. XU and W. KETTERLE. Evidence for superfluidity of ultracold fermions in an optical lattice. *Nature* **443** (2006) 961.

[Chi10] C. CHIN, R. GRIMM, P. S. JULIENNE and E. TIESINGA. Feshbach resonances in ultracold gases. *Rev. Mod. Phys.* In press.

[Cla07] B. CLANCY, L. LUO and J. E. THOMAS. Observation of Nearly Perfect Irrotational Flow in Normal and Superfluid Strongly Interacting Fermi Gases. *Phys. Rev. Lett.* **99** (2007) 140401.

[Clo62] A. M. CLOGSTON. Upper limit for the critical field in hard superconductors. *Phys. Rev. Lett.* **9** (1962) 266.

[Com08] R. COMBESCOT and S. GIRAUD. Normal State of Highly Polarized Fermi Gases: Full Many-Body Treatment. *Phys. Rev. Lett.* **101** (2008) 050404.

[Coo56] L. N. COOPER. Bound Electron Pairs in a Degenerate Fermi Gas. *Phys. Rev* **104** (1956) 1189.

[CT77] C. COHEN-TANNOUDJI, B. DIU and F. LALOË. Quantum Mechanics (Wiley-VHC, Berlin, 1977).

[Der01] A. DEREVIANKO, J. F. BABB and A. DALGARNO. High-precision calculations of van der Waals coefficients for heteronuclear alkali-metal dimers. *Phys. Rev. A* **63** (2001) 052704.

[D'I08] J. P. D'INCAO and B. D. ESRY. Suppression of Molecular Decay in Ultracold Gases without Fermi Statistics. *Phys. Rev. Lett.* **100** (2008) 163201.

[Die02] K. DIECKMANN, C. A. STAN, S. GUPTA, Z. HADZIBABIC, C. H. SCHUNCK and W. KETTERLE. Decay of an Ultracold Fermionic Lithium Gas near a Feshbach Resonance. *Phys. Rev. Lett.* **89** (2002) 203201.

[Du08] X. DU, L. LUO, B. CLANCY and J. E. THOMAS. Observation of anomalous spin segregation in a trapped Fermi gas. *Phys. Rev. Lett.* **101** (2008) 150401.

[Du09] X. DU, Y. ZHANG and J. E. THOMAS. Inelastic collisions of a Fermi gas in the BEC-BCS crossover. *Phys. Rev. Lett.* **102** (2009) 250402.

[Eag69] D. M. EAGLES. Possible Pairing without Superconductivity at Low Carrier Concentrations in Bulk and Thin-Film Superconducting Semiconductors. *Phys. Rev* **186** (1969) 456.

[Edg09] J. EDGE and N. COOPER. Signature of the Fulde-Ferrell-Larkin-Ovchinnikov phase in the Collective Modes of a Trapped Ultracold Fermi Gas. *Phys. Rev. Lett.* **103** (2009) 065301.

[Eng97] J. ENGELBRECHT, M. RANDERIA and C. A. R. SÁ DE MELO. BCS to Bose crossover: Broken-symmetry state. *Phys. Rev. B* **55** (1997) 15153.

[Esc09] Y. N. M. D. ESCOBAR, P. G. MICKELSON, M. YAN, B. J. DESALVO, S. B. NAGEL and T. C. KILLIAN. Bose-Einstein Condensation of ^{84}Sr. *Phys. Rev. Lett.* **103** (2009) 200402.

[Esr01] B. D. ESRY, C. H. GREENE and H. SUNO. Threshold laws for three-body recombination. *Phys. Rev. A* **65** (2001) 010705(R).

[Fer06a] F. FERLAINO, C. D'ERRICO, G. ROATI, M. ZACCANTI, M. INGUSCIO and G. MODUGNO. Feshbach spectroscopy of a K-Rb atomic mixture. *Phys. Rev. A* **73** (2006) 040702.

[Fer06b] F. FERLAINO, C. D'ERRICO, G. ROATI, M. ZACCANTI, M. INGUSCIO, G. MODUGNO and A. SIMONI. Erratum: Feshbach spectroscopy of a K-Rb atomic mixture [Phys. Rev. A 73, 040702 (2006)]. *Phys. Rev. A* **74** (2006) 039903(E).

[For05] M. M. FORBES, E. GUBANKOVA, W. V. LIU and F. WILCZEK. Stability Criteria for Breached-Pair Superfluidity. *Phys. Rev. Lett.* **94** (2005) 017001.

[Fuc07] J. FUCHS, G. J. DUFFY, G. VEERAVALLI, P. DYKE, M. BARTENSTEIN, C. VALE, P. HANNAFORD and W. J. ROWLANDS. Molecular Bose-Einstein condensation in a versatile low power crossed dipole trap. *J. Phys. B: At. Mol. Opt. Phys.* **40** (2007) 4109.

[Fuk07] T. FUKUHARA, Y. TAKASU, M. KUMAKURA and Y. TAKAHASHI. Degenerate Fermi Gases of Ytterbium. *Phys. Rev. Lett.* **98** (2007) 030401.

[Ful64] P. FULDE and R. A. FERRELL. Superconductivity in a strong spin-exchange field. *Phys. Rev* **135** (1964) A550.

[Gio08] S. GIORGINI, L. P. PITAEVSKII and S. STRINGARI. Theory of ultracold atomic Fermi gases. *Rev. Mod. Phys.* **80** (2008) 1215.

[Gre03] M. GREINER, C. A. REGAL and D. S. JIN. Emergence of a molecular Bose–Einstein condensate from a Fermi gas. *Nature* **426** (2003) 537.

[Gre05] M. GREINER, C. A. REGAL and D. S. JIN. Probing the Excitation Spectrum of a Fermi Gas in the BCS-BEC Crossover Regime. *Phys. Rev. Lett.* **94** (2005) 070403.

[Gri00] R. GRIMM, M. WEIDEMÜLLER and Y. OVCHINNIKOV. Optical dipole traps for neutral atoms. *Adv. At. Mol. Opt. Phys.* **42** (2000) 95.

[Gri06] R. GRIMM. in Ref. [Ing08], pages 413–462 (2006).

[Ho04] T.-L. HO. Universal Thermodynamics of Degenerate Quantum Gases in the Unitarity Limit. *Phys. Rev. Lett.* **92** (2004) 090402.

[Hod05] E. HODBY, S. THOMPSON, C. A. REGAL, M. GREINER, A. WILSON, D. S. JIN, E. A. CORNELL and C. E. WIEMAN. Production efficiency of ultracold Feshbach molecules in bosonic and fermionic systems. *Phys. Rev. Lett.* **94** (2005) 120402.

[Huc09] J. HUCKANS, J. R. WILLIAMS, E. HAZLETT, R. W. STITES and K. M. O'HARA. Three-body recombination in a three-state Fermi gas with widely tunable interactions. *Phys. Rev. Lett.* **102** (2009) 165302.

[Ina08] Y. INADA, M. HORIKOSHI, S. NAKAJIMA, M. KUWATA-GONOKAMI, M. UEDA and T. MUKAIYAMA. Critical Temperature and Condensate Fraction of a Fermion Pair Condensate. *Phys. Rev. Lett.* **101** (2008) 180406.

[Ing99] M. INGUSCIO, W. KETTERLE and C. SALOMON (Eds.) Bose-Einstein Condensation in Atomic Gases (IOS Press, Amsterdam, 1999). Proceedings of the International School of Physics "Enrico Fermi", Course CXL, Varenna, 7-17 July 1998.

[Ing08] M. INGUSCIO, W. KETTERLE and C. SALOMON (Eds.) Ultra-cold Fermi Gases (IOS Press, Amsterdam, 2008). Proceedings of the International School of Physics "Enrico Fermi", Course CLXIV, Varenna, 20-30 June 2006.

[Ino04] S. INOUYE, J. GOLDWIN, M. L. OLSEN, C. TICKNOR, J. L. BOHN and D. S. JIN. Observation of Heteronuclear Feshbach Resonances in a Mixture of Bosons and Fermions. *Phys. Rev. Lett.* **93** (2004) 183201.

[Isk06] M. ISKIN and C. A. R. SÁ DE MELO. Two-Species Fermion Mixtures with Population Imbalance. *Phys. Rev. Lett.* **97** (2006) 100404.

[Isk07a] M. ISKIN and C. A. R. SÁ DE MELO. Superfluid and insulating phases of fermion mixtures in optical lattices. *Phys. Rev. Lett.* **99** (2007) 080403.

[Isk07b] M. ISKIN and C. A. R. SÁ DE MELO. Ultracold heteronuclear molecules and ferroelectric superfluids. *Phys. Rev. Lett.* **99** (2007) 110402.

[Isk08a] M. ISKIN and C. A. R. SÁ DE MELO. Fermi-Fermi mixtures in the strong-attraction limit. *Phys. Rev. A* **77** (2008) 013625.

[Isk08b] M. ISKIN and C. A. R. SÁ DE MELO. Quantum phases of Fermi-Fermi mixtures in optical lattices. *Phys. Rev. A* **78** (2008) 013607.

[Isk08c] M. ISKIN and C. J. WILLIAMS. Trap-imbalanced fermion mixtures. *Phys. Rev. A* **77** (2008) 013605.

[Joc03] S. JOCHIM, M. BARTENSTEIN, A. ALTMEYER, G. HENDL, S. RIEDL, C. CHIN, J. HECKER DENSCHLAG and R. GRIMM. Bose-Einstein Condensation of Molecules. *Science* **302** (2003) 2101.

[Joc04] S. JOCHIM. Bose-Einstein Condensation of Molecules. Ph.D. thesis, Universität Innsbruck (2004).

[Jos07] J. JOSEPH, B. CLANCY, L. LUO, J. KINAST, A. TURLAPOV and J. E. THOMAS. Measurement of Sound Velocity in a Fermi Gas near a Feshbach Resonance. *Phys. Rev. Lett.* **98** (2007) 170401.

[Kin05] J. KINAST, A. TURLAPOV, J. E. THOMAS, Q. CHEN and J. STAJIC. Heat Capacity of a Strongly Interacting Fermi Gas. *Science* **307** (2005) 1296.

[Köh06] T. KÖHLER and K. GÓRAL. Production of cold molecules via magnetically tunable Feshbach resonances. *Rev. Mod. Phys.* **78** (2006) 1311.

[Kon64] J. KONDO. Resistance minimum in dilute magnetic alloys. *Prog. Theor. Phys* **32** (1964) 37.

[Lah09] T. LAHAYE, C. MENOTTI, L. SANTOS, M. LEWENSTEIN and T. PFAU. The physics of dipolar bosonic quantum gases. *Rep. Prog. Phys.* **72** (2009) 126401.

[Lar65] A. I. LARKIN and Y. N. OVCHINNIKOV. Inhomogeneous state of superconductors. *Sov. Phys. JETP* **20** (1965) 762.

[LeB07] L. LEBLANC and J. H. THYWISSEN. Species-specific optical lattices. *Phys. Rev. A* **75** (2007) 053612.

[Leg80] A. J. LEGGETT. Modern Trends in the Theory of Condensed Matter, vol. 115 of *Lecture Notes in Physics, 13* (Springer Verlag, Berlin, 1980).

[Lev09] J. LEVINSEN, T. G. TIECKE, J. T. M. WALRAVEN and D. S. PETROV. Atom-dimer scattering and long-lived trimers in fermionic mixtures. *Phys. Rev. Lett.* **103** (2009) 153202.

[Lia09] Y. LIAO, A. S. C. RITTNER, T. PAPROTTA, W. LI, G. B. PARTRIDGE, R. G. HULET, S. K. BAUR and E. J. MUELLER. Spin-Imbalance in a One-Dimensional Fermi Gas. *arXiv:0912.0092* .

[Liu03] W. V. LIU and F. WILCZEK. Interior Gap Superfluidity. *Phys. Rev. Lett.* **90** (2003) 47002.

[Lob06] C. LOBO, A. RECATI, S. GIORGINI and S. STRINGARI. Normal State of a Polarized Fermi Gas at Unitarity. *Phys. Rev. Lett.* **97** (2006) 200403.

[Luo07] L. LUO, B. CLANCY, J. JOSEPH, J. KINAST and J. E. THOMAS. Measurement of the Entropy and Critical Temperature of a Strongly Interacting Fermi Gas. *Phys. Rev. Lett.* **98** (2007) 080402.

[Luo09] L. LUO and J. E. THOMAS. Thermodynamic Measurements in a Strongly Interacting Fermi Gas. *J. Low Temp. Phys.* **154** (2009) 1.

[McN06] J. M. MCNAMARA, T. JELTES, A. S. TYCHKOV, W. HOGERVORST and W. VASSEN. Degenerate Bose-Fermi mixture of metastable atoms. *Phys. Rev. Lett.* **97** (2006) 080404.

[Met99] H. J. METCALF and P. VAN DER STRATEN. Laser Cooling and Trapping (Springer, New York, 1999).

[Mil07] D. E. MILLER, J. K. CHIN, C. A. STAN, Y. LIU, W. SETIAWAN, C. SANNER and W. KETTERLE. Critical Velocity for Superfluid Flow across the BEC-BCS Crossover. *Phys. Rev. Lett.* **99** (2007) 070402.

[Moe95] A. J. MOERDIJK, B. J. VERHAAR and A. AXELSSON. Resonances in ultracold collisions of ^{6}Li, ^{7}Li, and ^{23}Na. *Phys. Rev. A* **51** (1995) 4852.

[Mor09] C. MORA and F. CHEVY. Ground state of a tightly bound composite dimer immersed in a Fermi Sea. *Phys. Rev. A* **80** (2009) 033607.

[Mud02] M. MUDRICH, S. KRAFT, K. SINGER, R. GRIMM, A. P. MOSK and M. WEIDEMÜLLER. Sympathetic Cooling with Two Atomic Species in an Optical Trap. *Phys. Rev. Lett.* **88** (2002) 253001.

[Nai10] D. NAIK, A. TRENKWALDER, F. SPIEGELHALDER, C. KOHSTALL, G. HENDL, F. SCHRECK and R. GRIMM **in preparation**.

[Nas09] S. NASCIMBÈNE, N. NAVON, K. J. JIANG, F. CHEVY and C. SALOMON. Exploring the thermodynamics of a universal Fermi gas. *arXiv:0911.0747* .

[Nis08] Y. NISHIDA and S. TAN. Universal Fermi Gases in Mixed Dimensions. *Phys. Rev. Lett.* **101** (2008) 170401.

[Nis09a] Y. NISHIDA. Induced p-wave superfluidity in two dimensions: Brane world in cold atoms and nonrelativistic defects CFTs. *Ann. Phys* **324** (2009) 897.

[Nis09b] Y. NISHIDA and S. TAN. Confinement-induced Efimov resonances in Fermi-Fermi mixtures. *Phys. Rev. A* **79** (2009) 060701(R).

[Noz85] P. NOZIERES and S. SCHMITT-RINK. Bose condensation in an attractive fermion gas: From weak to strong coupling superconductivity. *J. Low Temp. Phys.* **59** (1985) 195.

[O'H02] K. M. O'HARA, S. HEMMER, M. E. GEHM, S. R. GRANADE and J. E. THOMAS. Observation of a Strongly Interacting Degenerate Fermi Gas of Atoms. *Science* **298** (2002) 2179.

[Ors08] G. ORSO, L. P. PITAEVSKII and S. STRINGARI. Equilibrium and dynamics of a trapped superfluid Fermi gas with unequal masses. *Phys. Rev. A* **77** (2008) 033611.

[Ott08] T. B. OTTENSTEIN, T. LOMPE, M. KOHNEN, A. N. WENZ and S. JOCHIM. Collisional stability of a three-component degenerate Fermi gas. *Phys. Rev. Lett.* **101** (2008) 203202.

[Paa06] T. PAANANEN, J.-P. MARTIKAINEN and P. TÖRMÄ. Pairing in a three-component Fermi gas. *Phys. Rev. A* **73** (2006) 053606.

[Par05] G. B. PARTRIDGE, K. E. STRECKER, R. I. KAMAR, M. W. JACK and R. G. HULET. Molecular Probe of Pairing in the BEC-BCS Crossover. *Phys. Rev. Lett.* **95** (2005) 020404.

[Par06] G. B. PARTRIDGE, W. LI, R. I. KAMAR, Y. AN LIAO and R. G. HULET. Pairing and phase separation in a polarized Fermi gas. *Science* **311** (2006) 503.

[Pet04] D. S. PETROV, C. SALOMON and G. V. SHLYAPNIKOV. Weakly Bound Dimers of Fermionic Atoms. *Phys. Rev. Lett.* **93** (2004) 090404.

[Pet05] D. S. PETROV, C. SALOMON and G. V. SHLYAPNIKOV. Diatomic molecules in ultracold Fermi gases – novel composite bosons. *J. Phys. B: At. Mol. Opt. Phys.* **38** (2005) S645.

[Pet07] D. S. PETROV, G. E. ASTRAKHARCHIK, D. J. PAPOULAR, C. SALOMON and G. V. SHLYAPNIKOV. Crystalline Phase of Strongly Interacting Fermi Mixtures. *Phys. Rev. Lett.* **99** (2007) 130407.

[Pro08] N. PROKOF'EV and B. SVISTUNOV. Bold diagrammatic Monte Carlo: A generic sign-problem tolerant technique for polaron models and possibly interacting many-body problems. *Phys. Rev. B* **77** (2008) 125101.

[Reg03a] C. A. REGAL, C. TICKNOR, J. L. BOHN and D. S. JIN. Creation of ultracold molecules from a Fermi gas of atoms. *Nature* **424** (2003) 47.

[Reg03b] C. A. REGAL, C. TICKNOR, J. L. BOHN and D. S. JIN. Tuning p-Wave Interactions in an Ultracold Fermi Gas of Atoms. *Phys. Rev. Lett.* **90** (2003) 053201.

[Reg04] C. A. REGAL, M. GREINER and D. S. JIN. Observation of Resonance Condensation of Fermionic Atom Pairs. *Phys. Rev. Lett.* **92** (2004) 040403.

[Reg05a] C. REGAL. Experimental realization of BCS-BEC crossover physics with a Fermi gas of atoms. Ph.D. thesis, University of Colorado (2005).

[Reg05b] C. A. REGAL, M. GREINER, S. GIORGINI, M. HOLLAND and D. S. JIN. Momentum Distribution of a Fermi Gas of Atoms in the BCS-BEC Crossover. *Phys. Rev. Lett.* **95** (2005) 250404.

[Rie08] S. RIEDL, E. R. SÁNCHEZ GUAJARDO, C. KOHSTALL, A. ALTMEYER, M. J. WRIGHT, J. HECKER DENSCHLAG, R. GRIMM, G. M. BRUUN and H. SMITH. Collective oscillations of a Fermi gas in the unitarity limit: Temperature effects and the role of pair correlations. *Phys. Rev. A* **78** (2008) 053609.

[Sal07] H. SALAMI, A. J. ROSS, P. CROZET and W. JASTRZEBSKI. A full analytic potential energy curve for the a Σ state of KLi from a limited vibrational data set. *J. Chem. Phys.* **126** (2007) 194313.

[Sar63] G. SARMA. On the influence of a uniform exchange field acting on the spins of the conduction electrons in a superconductor. *J. Phys. Chem. Sol.* **24** (1963) 1029.

[Sch01] F. SCHRECK, L. KHAYKOVICH, K. L. CORWIN, G. FERRARI, T. BOURDEL, J. CUBIZOLLES and C. SALOMON. Quasipure Bose-Einstein condensate immersed in a Fermi sea. *Phys. Rev. Lett.* **87** (2001) 080403.

[Sch05] C. H. SCHUNCK, M. W. ZWIERLEIN, C. A. STAN, S. M. F. RAUPACH, W. KETTERLE, A. SIMONI, E. TIESINGA, C. J. WILLIAMS and P. S. JULIENNE. Feshbach resonances in fermionic ^{6}Li. *Phys. Rev. A* **71** (2005) 045601.

[Sch07] C. H. SCHUNCK, M. W. ZWIERLEIN, A. SCHIROTZEK and W. KETTERLE. Superfluid Expansion of a Rotating Fermi Gas. *Phys. Rev. Lett.* **98** (2007) 050404.

[Sch08a] A. SCHIROTZEK, Y.-I. SHIN, C. H. SCHUNCK and W. KETTERLE. Determination of the Superfluid Gap in Atomic Fermi Gases by Quasiparticle Spectroscopy. *Phys. Rev. Lett.* **101** (2008) 140403.

[Sch08b] C. H. SCHUNCK, Y.-I. SHIN, A. SCHIROTZEK and W. KETTERLE. Determination of the fermion pair size in a resonantly interacting superfluid. *Nature* **454** (2008) 739.

[Sch09] A. SCHIROTZEK, C.-H. WU, A. SOMMER and M. W. ZWIERLEIN. Observation of Fermi Polarons in a Tunable Fermi Liquid of Ultracold Atoms. *Phys. Rev. Lett.* **102** (2009) 230402.

[Shi06] Y.-I. SHIN, M. W. ZWIERLEIN, C. H. SCHUNCK, A. SCHIROTZEK and W. KETTERLE. Observation of Phase Separation in a Strabismicongly Interacting Imbalanced Fermi Gas. *Phys. Rev. Lett.* **97** (2006) 030401.

[Shi07] Y.-I. SHIN, C. H. SCHUNCK, A. SCHIROTZEK and W. KETTERLE. Tomographic rf Spectroscopy of a Trapped Fermi Gas at Unitarity. *Phys. Rev. Lett.* **99** (2007) 090403.

[Shi08] Y.-I. SHIN, C. H. SCHUNCK, A. SCHIROTZEK and W. KETTERLE. Phase diagram of a two-component Fermi gas with resonant interactions. *Nature* **451** (2008) 689.

[Sim03] A. SIMONI, F. FERLAINO, G. ROATI, G. MODUGNO and M. INGUSCIO. Magnetic Control of the Interaction in Ultracold K-Rb Mixtures. *Phys. Rev. Lett.* **90** (2003) 163202.

[Spi09] F. M. SPIEGELHALDER, A. TRENKWALDER, D. NAIK, G. HENDL, F. SCHRECK and R. GRIMM. Collisional Stability of ^{40}K Immersed in a Strongly Interacting Fermi Gas of ^{6}Li. *Phys. Rev. Lett.* **103** (2009) 223203.

[Spi10] F. SPIEGELHALDER, A. TRENKWALDER, D. NAIK, G. KERNER, E. WILLE, G. HENDL, F. SCHRECK and R. GRIMM. All-optical production of a degenerate mixture of ^{6}Li and ^{40}K and creation of heteronuclear molecules. *arXiv:1001.5253* .

[Sta04] C. A. STAN, M. W. ZWIERLEIN, C. H. SCHUNCK, S. M. F. RAUPACH and W. KETTERLE. Observation of Feshbach Resonances between Two Different Atomic Species. *Phys. Rev. Lett.* **93** (2004) 143001.

[Ste06] J. T. STEWART, J. P. GAEBLER, C. A. REGAL and D. S. JIN. Potential Energy of a ^{40}K Fermi Gas in the BCS-BEC Crossover. *Phys. Rev. Lett.* **97** (2006) 220406.

[Ste08] J. T. STEWART, J. P. GAEBLER and D. S. JIN. Using photoemission spectroscopy to probe a strongly interacting Fermi gas. *Nature* **454** (2008) 744.

[Ste09] S. STELLMER, M. K. TEY, B. HUANG, R. GRIMM and F. SCHRECK. Bose-Einstein Condensation of Strontium. *Phys. Rev. Lett.* **103** (2009) 200401.

[Sto88] H. T. C. STOOF, J. KOELMAN and B. J. VERHAAR. Spin-exchange and dipole relaxation rates in atomic hydrogen: Rigorous and simplified calculations. *Phys. Rev. B* **38** (1988) 4688.

[Str03] K. E. STRECKER, G. B. PARTRIDGE and R. G. HULET. Conversion of an atomic Fermi gas to a long-lived molecular Bose gas. *Phys. Rev. Lett.* **91** (2003) 080406.

[Tag08] M. TAGLIEBER, A.-C. VOIGT, T. AOKI, T. W. HÄNSCH and K. DIECKMANN. Quantum degenerate two-species Fermi-Fermi mixture coexisting with a Bose-Einstein condensate. *Phys. Rev. Lett.* **100** (2008) 010401.

[Tie09] T. G. TIECKE. Feshbach resonances in ultracold mixtures of the fermionic quantum gases ^{6}Li and ^{40}K. Ph.D. thesis, University of Amsterdam (2009).

[Tie10] T. G. TIECKE, M. R. GOOSEN, A. LUDEWIG, S. D. GENSEMER, S. KRAFT, S. J. J. M. F. KOKKELMANS and J. T. M. WALRAVEN. Broad Feshbach Resonance in the ^{6}Li-^{40}K Mixture. *Phys. Rev. Lett.* **104** (2010) 053202.

[Tim99] E. TIMMERMANS, P. TOMMASINI, M. HUSSEIN and A. J. KERMAN. Feshbach resonances in atomic Bose-Einstein condensates. *Phys. Rep.* **315** (1999) 199.

[Vee08] G. VEERAVALLI, E. KUHNLE, P. DYKE and C. VALE. Bragg Spectroscopy of a Strongly Interacting Fermi Gas. *Phys. Rev. Lett.* **101** (2008) 250403.

[Voi09] A.-C. VOIGT, M. TAGLIEBER, L. COSTA, T. AOKI, W. WIESER, T. W. HÄNSCH and K. DIECKMANN. Ultracold Heteronuclear Fermi-Fermi Molecules. *Phys. Rev. Lett.* **102** (2009) 020405.

[Wan09] B. WANG, H.-D. CHEN and S. D. SARMA. Quantum phase diagram of fermion mixtures with population imbalance in one-dimensional optical lattices. *Phys. Rev. A* **79** (2009) 051604(R).

[Wen09] A. N. WENZ, T. LOMPE, T. B. OTTENSTEIN, F. SERWANE, G. ZÜRN and S. JOCHIM. Universal trimer in a three-component Fermi gas. *Phys. Rev. A* **80** (2009) 040702(R).

[Wil08] E. WILLE, F. M. SPIEGELHALDER, G. KERNER, D. NAIK, A. TRENKWALDER, G. HENDL, F. SCHRECK, R. GRIMM, T. G. TIECKE, J. T. M. WALRAVEN, S. J. J. M. F. KOKKELMANS, E. TIESINGA and P. S. JULIENNE. Exploring an Ultracold Fermi-Fermi Mixture: Interspecies Feshbach Resonances and Scattering Properties of ^{6}Li and ^{40}K. *Phys. Rev. Lett.* **100** (2008) 053201.

[Wil09a] E. WILLE. Preparation of an Optically Trapped Fermi-Fermi Mixture of ^{6}Li and ^{40}K Atoms and Characterization of the Interspecies Interactions by Feshbach Spectroscopy. Ph.D. thesis, Innsbruck University (2009).

[Wil09b] J. R. WILLIAMS, E. HAZLETT, J. HUCKANS, R. W. STITES, Y. ZHANG and K. M. O'HARA. Evidence for an excited-state Efimov trimer in a three-component Fermi gas. *Phys. Rev. Lett.* **103** (2009) 130404.

[Zha04] J. ZHANG, E. G. M. VAN KEMPEN, T. BOURDEL, L. KHAYKOVICH, J. CUBIZOLLES, F. CHEVY, M. TEICHMANN, L. TARRUELL, S. J. J. M. F. KOKKELMANS and C. SALOMON. *P*-wave Feshbach resonances of ultracold ^{6}Li. *Phys. Rev. A* **70** (2004) 030702(R).

[Zwi03] M. W. ZWIERLEIN, S. M. F. RAUPACH, S. GUPTA, Z. HADZIBABIC and W. KETTERLE. Observation of Bose-Einstein Condensation of Molecules. *Phys. Rev. Lett.* **91** (2003) 250401.

[Zwi04] M. W. ZWIERLEIN, C. A. STAN, C. H. SCHUNCK, S. M. F. RAUPACH, A. J. KERMAN and W. KETTERLE. Condensation of Pairs of Fermionic Atoms near a Feshbach Resonance. *Phys. Rev. Lett.* **92** (2004) 120403.

[Zwi05a] M. W. ZWIERLEIN, J. R. ABO-SHAEER, A. SCHIROTZEK, C. H. SCHUNCK and W. KETTERLE. Vortices and superfluidity in a strongly interacting Fermi gas. *Nature* **435** (2005) 1047.

[Zwi05b] M. W. ZWIERLEIN, C. H. SCHUNCK, C. A. STAN, S. M. F. RAUPACH and W. KETTERLE. Formation Dynamics of a Fermion Pair Condensate. *Phys. Rev. Lett.* **94** (2005) 180401.

[Zwi06] M. W. ZWIERLEIN, A. SCHIROTZEK, C. H. SCHUNCK and W. KETTERLE. Fermionic Superfluidity with Imbalanced Spin Populations. *Science* **311** (2006) 492.